Long noncoding RNA *lncMREF* promotes myogenic differentiation and muscle regeneration by interacting with the Smarca5/p300 complex

Wei Lv[1,2,3,†], **Wei Jiang**[1,2,†], **Hongmei Luo**[1,2], **Qian Tong**[1,2], **Xiaoyu Niu**[1,2], **Xiao Liu**[1,2,4], **Yang Miao**[1,2], **Jingnan Wang**[1,2], **Yiwen Guo**[1,2], **Jianan Li**[1,2], **Xizhen Zhan**[1,2], **Yunqing Hou**[1,2], **Yaxin Peng**[1,2], **Jian Wang**[1,2,4], **Shuhong Zhao** [1,2,3,5,6], **Zaiyan Xu**[1,4] **and Bo Zuo** [1,2,3,5,6,*]
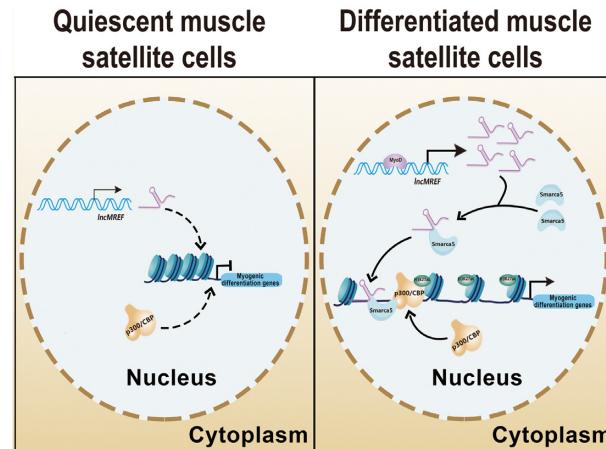
[1]Key Laboratory of Swine Genetics and Breeding of the Ministry of Agriculture and Rural Affairs, Huazhong Agricultural University, Wuhan, China, [2]Key Laboratory of Agriculture Animal Genetics, Breeding and Reproduction of the Ministry of Education, Huazhong Agricultural University, Wuhan, China, [3]Hubei Hongshan Laboratory, Wuhan, China, [4]Department of Basic Veterinary Medicine, College of Veterinary Medicine, Huazhong Agricultural University, Wuhan, China, [5]The Cooperative Innovation Center for Sustainable Pig Production, Wuhan, China and [6]Frontiers Science Center for Animal Breeding and Sustainable Production, Wuhan, China

ABSTRACT

Long noncoding RNAs (lncRNAs) play important roles in the spatial and temporal regulation of muscle development and regeneration. Nevertheless, the determination of their biological functions and mechanisms underlying muscle regeneration remains challenging. Here, we identified a lncRNA named *lncMREF* (lncRNA muscle regeneration enhancement factor) as a conserved positive regulator of muscle regeneration among mice, pigs and humans. Functional studies demonstrated that *lncMREF*, which is mainly expressed in differentiated muscle satellite cells, promotes myogenic differentiation and muscle regeneration. Mechanistically, *lncMREF* interacts with Smarca5 to promote chromatin accessibility when muscle satellite cells are activated and start to differentiate, thereby facilitating genomic binding of p300/CBP/H3K27ac to upregulate the expression of myogenic regulators, such as MyoD and cell differentiation. Our results unravel a novel temporal-specific epigenetic regulation during muscle regeneration and reveal that *lncMREF*/Smarca5-mediated epigenetic programming is responsible for muscle cell differentiation, which provides new insights into the regulatory mechanism of muscle regeneration.

GRAPHICAL ABSTRACT

INTRODUCTION

Skeletal muscle has a significant ability to regenerate in the event of injury or other external stimuli. Muscle repair is a highly coordinated process involving muscle injury, regeneration, and muscle fiber remodeling ([1–3]). Muscle regeneration starts with the activation and expansion of muscle stem cells (satellite cells), which reside in the basal layer of muscle fibers, differentiate and finally fuse into multinucleated myotubes ([4,5]). At the final stage of muscle repair, myotubes undergo hypertrophy and remodeling to generate mature muscle fibers and restore their contractility ([6]). The process of muscle regeneration is regulated not only by a family of muscle-restricted basic helix–loop–helix transcription fac-

---

*To whom correspondence should be addressed. Tel: +86 027 8728 2091; Fax: +86 027 8728 0408; Email: zuobo@mail.hzau.edu.cn
†The authors wish it to be known that, in their opinion, the first two authors should be regarded as Joint First Authors.

tors, such as Myf5, MyoD and myogenin (MyoG), but also by various epigenetic regulations. Epigenetic regulations mainly include (i) chromatin remodeling, (ii) posttranslational reversible modifications of histones, such as methylation, acetylation, phosphorylation and ubiquitination, (iii) DNA methylation and demethylation and (iv) noncoding RNA regulation (7). Dissecting the regulatory network of muscle regeneration is of great importance for the treatment of human muscle diseases and improvement of animal meat production.

Eukaryotic chromatin is the material basis of all genetic processes, and dynamic changes in chromatin configuration are key factors in the regulation of gene expression. Chromatin remodeling complexes are divided into four major categories: SWI/SNF, CHD, ISWI and INO80 (8–11). The SWI/SNF complex is the most studied chromatin remodeling complex in mammals and has been found to be involved in various life activities (12). This complex has ~15 subunits, each of which is transcribed and translated from a separate gene (13). Smarca5 (also known as Snf2 h), which belongs to the SWI/SNF family, is an important enzyme with remodeling activity (14,15). Smarca5 functions as a molecular motor for nuclear complexes and is indispensable for hematopoiesis in the developing embryos and later in the fetuses (16,17). Chromatin remodeling is often accompanied by histone modifications, such as acetylation and methylation. Acetylation of lysine residues of histones H3 and H4 (H3K27ac, H4K16ac, H3K9ac, H4K4ac) and trimethylation of lysine 4 of histones H3 and H4 (H3K4me3, H4K4me3) are associated with open chromatin state and transcriptional activation, whereas trimethylation of lysine 27 of histone H3 (H3K27me3), the 2/3 methylation of lysine 9 of histone H3 (H3K9me2/3) and 2/3 methylation of lysine 20 of histone H4 (H4K20me2/3) are associated with transcriptional repression (18). Many studies have shown that chromatin remodeling and histone modification play important roles in epigenetic regulation of muscle development and regeneration. For example, E1A binding protein p300 (p300), which is a key histone acetyltransferase in the nucleus, promotes myogenic differentiation by increasing H3K27ac levels (19–22).

Long noncoding RNAs (lncRNAs) are a class of RNAs >200 nucleotides in length and do not encode functional proteins (23). Compared with protein-coding genes, the expression and regulatory networks of lncRNAs are more spatially and temporally specific. To date, thousands of lncRNAs have been identified in skeletal muscles by high-throughput sequencing, but only a few of them have been verified to function in muscle development and regeneration (24); these lncRNAs mainly include *H19* (25), *SYISL* (26), *Linc-RAM* (27), *linc-MD1* (28), *lnc-mg* (29), *m1/2sbsRNAs* (30), *Dum* (31), *lncMyoD (32)*, *MAR1* (33), *lncIRS1* (34), *lncMGPF* (35) and so on. These lncRNAs play roles in myogenesis through multiple regulatory mechanisms, such as chromatin modification (36), transcription activation (37), microRNA sponging (28), and mRNA splicing and translation (38). Here, we identified a novel lncRNA named lncRNA muscle regeneration enhancement factor (*lncMREF*) as a positive regulator of muscle regeneration. *lncMREF* is mainly expressed in differentiated skeletal muscle

satellite cells, and *lncMREF* overexpression promotes myogenic differentiation. *lncMREF* knockout in mice does not affect normal muscle growth but leads to a significant decrease in muscle regeneration. Mechanistic analyses showed that *lncMREF* recruits Smarca5 and p300/CBP to upregulate chromatin accessibility and myogenic gene expression, and thereby promotes the differentiation of muscle satellite cells and muscle regeneration.

MATERIALS AND METHODS

Animals

All procedures involving animals were performed in accordance with good laboratory practice guidelines, and animals were provided with nutritious food and adequate water. Animal feeding and testing were based on National Research Council Guide for the Care and Use of Laboratory Animals and approved by the Institutional Animal Care and Use Committee at Huazhong Agricultural University. Piglets were slaughtered according to standard procedures in accordance with the guidelines in the Regulations of the Standing Committee of the Hubei Provincial People's Congress (Hubei Province, China, HZAUSW-2017-008). All mice were obtained from the Experimental Animal Center of Huazhong Agricultural University. All pigs were obtained from the Experimental Pig Farm of Huazhong Agricultural University.

Isolation and culture of skeletal muscle satellite cells

Mouse skeletal muscle satellite cells were isolated from 5-week-old C57BL mice; pig skeletal muscle satellite cells were isolated from 1-day-old Large White male piglets. Skeletal muscle satellite cells were isolated and cultured as previously described (39,40). Briefly, muscle was minced and treated with 2 mg/ml type I collagenase (C0130; Sigma Aldrich, St. Louis, MO, USA). Digestion was stopped by RPMI 1640 medium containing 20% fetal bovine serum (FBS). Cells were cultured at $37°C$ and $5\% CO_2$ in growth medium (RPMI 1640 supplemented with 20% FBS, 4 ng/ml basic fibroblast growth factor, 1% chicken embryo extract, and 1% penicillin-streptomycin) on collagen-coated cell culture plates. Freshly isolated satellite cells (FISCs) were cultured in growth medium for 24 h (Activated satellite cells, ASCs) or 72 h (Differentiated satellite cells, DSCs) (41). C2C12 myogenic cells, porcine kidney cells, 293T cells and HeLa cells were obtained from Chinese Academy of Sciences cell bank and grown in an incubator at $37°C$ and $5\% CO_2$, and proliferating cells were cultured in Dulbecco's modified Eagle's medium (DMEM) supplemented with 10% FBS (Gibco, Grand Island, NY, USA). Human skeletal muscle myogenic cells (Cat#3501) were obtained from ScienCell Research Laboratories and cultured at $37°C$ and $5\% CO_2$ and proliferating cells were cultured in DMEM supplemented with 5% FBS (Gibco, Grand Island, NY, USA). For myogenic differentiation, cells were cultured in DMEM containing 2% horse serum (Gibco). Pig fibroblasts were isolated from 25-day-old Large White pig fetuses and cultured in DMEM supplemented with 15% of FBS (Gibco, Grand Island, NY, USA).

Total RNA extraction and quantitative real-time PCR

Total RNA was isolated using TRIzol reagent (Invitrogen, USA) according to the manufacturer's instructions. Total RNA was reverse-transcribed using RevertAid Reverse Transcriptase (Thermo Scientific, USA). Quantitative real-time PCR (qRT-PCR) analyses were performed using the Applied Biosystems StepOnePlus real-time PCR system. Relative RNA expression was calculated using the Ct ($2^{-\Delta\Delta Ct}$) method (42). All primers used in qRT-PCR are presented in Supplementary Materials, Table S1.

Rapid amplification of complementary DNA ends (RACE)

We performed 5′ and 3′ RACE using the Takara SMARTer RACE complementary DNA amplification Kit (Clontech, USA) according to the manufacturer's instructions. The sequences of gene-specific primers used for *lncMREF* of mouse, pig and human RACE are presented in Supplementary Materials, Table S2.

RNA fluorescence in situ hybridization (FISH)

FISH was performed using the lncRNA FISH Kit (Guangzhou RiboBio, China) according to the manufacturer's instructions. Briefly, cells were fixed with 4% formaldehyde for 10 min at room temperature. After washing, cells were permeabilized with 0.5% Triton X-100 for 30 min at 37°C. Next, cells were incubated with RNA probes in hybridization buffer overnight at 37°C. The RNA probes were directly conjugated with a fluorophore. Then, the cells were washed three times with saline sodium citrate buffer, stained with 4′,6-diamidino-2-phenylindole.

Nuclear and cytoplasmic RNA fractionation

Nuclear and cytoplasmic RNA fractionation was performed according to a previously published method (27), and distribution quantification was analyzed via qRT-PCR. The nuclear and cytoplasmic distribution was determined by qRT-PCR according to the published literature (43,44). All primers used in qRT-PCR are presented in Supplementary Materials, Table S1.

Small interfering RNA synthesis and cell transfection

Small interfering RNAs (siRNAs) targeting *lncMREF*, *Smarca5* and *p300* were synthesized by Genepharma (Genepharma, China); all siRNA sequences are presented in Supporting Information, Table S2. For cell transfection, we transfected C2C12 myoblasts, human skeletal muscle myoblasts, and mouse and pig myogenic progenitor cells with ∼160 μM siRNA oligonucleotides using 9 μl Lipofectamine 2000 (Invitrogen, USA) in each well of a six-well plate.

Lentivirus packaging and infection

To construct lentivirus-mediated overexpression vectors for *lncMREF*, *plncMREF* and *hlncMREF*, sequences of *lncMREF*, *plncMREF* and *hlncMREF* were separately subcloned into the lentivirus vector PCDH-CMV-copGFP (Addgene, USA). We packaged the lentivirus in 293T cells using three vectors: 10.7 μg pLKO.1-TRC or PCDH-CMV-copGFP, 8.0 μg psPAX2 (Addgene, USA), and 5.3 μg PDM2.G (Addgene, USA). For lentivirus infection of cells, 10 μl virus and 1 μg polybrene were added to each milliliter of medium and then was replaced with fresh medium after 24 h. For mouse muscle infection, we injected 50 μl *lncMREF*, *plncMREF* or *hlncMREF* overexpression lentivirus vector and empty lentivirus vector into the Gas muscles of the left and right legs, respectively, of five 1-month-old wild-type (WT) mice or Mdx mice every 7 days. The lentivirus concentration used in all the assays was above 1×10^8 transducing units per milliliter. The multiplicity of infection was 10, 15 and 25 plaque forming unit per cell for the infections of C2C12 myoblasts, pig myogenic progenitor cells, and human skeletal muscle myoblasts, respectively. All primers used for plasmid construction and lentivirus production are presented in Supplementary Materials Table S3.

Plasmid construction and transfection

To construct the *lncMREF*, p300 and *Smarca5* overexpression plasmids, the full-length or coding sequences of *lncMREF*, *p300* and *Smarca5* were cloned into the pcDNA3.1 plasmid (Addgene, USA). For *in vitro* transcription assays, full-length and truncated fragments of *lncMREF* were cloned into the pGEM-3Z vector (Promega, USA). Full-length sequences of *lncMREF*, *p300* and *Smarca5* were amplified using specific F/R primers (Supplementary Materials, Table S3). For cell transfection, we transfected C2C12 myoblasts, human skeletal muscle myoblasts, and mouse myogenic progenitor cells with approximately 4 μg plasmid using 9 μl Lipofectamine 2000 (Invitrogen, USA) in each well of a 6-well plate.

Western blotting

Proteins were extracted from muscle tissues and cells using radioimmunoprecipitation assay buffer with 1% (v/v) phenylmethylsulfonyl fluoride (Beyotime Biotechnology, China). Western blotting was performed according to a previously reported method (45). The antibody specific information is in the supplemental materials. All protein levels were normalized to the housekeeping protein β-actin, and densitometric quantification of the Western blotting bands was performed using ImageJ software. Antibody details are presented in Supplementary Materials, Table S4.

Cell immunofluorescence staining

Cell immunofluorescence staining was performed according to a previously published method (25). Immunofluorescence staining antibodies included Pax7, MyoD, Smarca5, p300, MyHC, MyoG, EGFP, eMyHC and Dystrophin. Antibody details are presented in Supporting Information, Table S4. DAPI was used to visualize cell nuclei with a fluorescence microscope (DP80; Olympus, Japan).

Generation of *lncMREF* knockout mice and measurement of phenotypes

We generated *lncMREF* knockout (KO) mice using the CRISPR genome-editing system with the

C57BL/6 background according to a previous report (46). Two single-guide RNAs (sgRNAs) (sgRNA1: 5′-CCAAGTACCGCAATCCCAGACCA-3′; sgRNA2: 5′-AAACCAACATCTCAGGCGATTGG-3′) were designed using an online CRISPR design tool (http://tools.geneome-engineering.org) to delete the 819 bp genomic region containing the complete *lncMREF* transcript, and these sgRNAs were inserted into the px459 vector (Addgene, USA). The purified sgRNA-Cas9-px459 vector was injected into fertilized eggs, and successful KO was validated through PCR amplification with the specific primers (F: 5′-GGCTGTGATGGGTTTATTGATGGG-3′; R: 5′-TAGGTAGTTTACAAGGCTGGACGTTACC-3′) and sequencing. Wild type (WT) mice had an amplicon size of 1074 bp, whereas KO mice possessed an amplicon of only 264 bp. The founder mice were randomly mated to produce offspring for further experiments. Male and female KO and WT offspring mice were randomly selected and their body weights were measured weekly. The whole legs, Gas, transverse abdominal (TA), and Qu muscles of KO and WT mice were collected and weighed at 2 months of age. Three qRT-PCR primers targeting exon 1, exon 2 and exons 1–2, respectively, were used to detect both alleles in muscle tissue of WT, heterozygous and KO mice. The three primers are presented in Supplementary Materials, Table S1.

Histology staining

Hematoxylin and eosin (HE) staining of muscle sections was performed according to a previously reported method (29) and visualized using an optical microscope (BX53; Olympus, Japan). The cross-sectional areas of individual myofibres were quantified using ImageJ software. Immunohistochemical staining was performed as described previously (47) and visualized using a confocal laser scanning microscope (LSM800; Zeiss, Germany). For immunofluorescence staining, samples were repaired in 0.01 M sodium citrate solution (pH 6.0) for 30 min at 70°C, and incubated in blocking buffer (5% goat serum, 2% bovine serum albumin, 0.1% Triton X-100 and 0.1% sodium azide in phosphate-buffered saline) for 2 h. Samples were then incubated with primary antibodies diluted in blocking buffer overnight at 4°C. After washing with phosphate-buffered saline, the samples were incubated with secondary antibodies for 1 h at 37°C. At last, the samples were incubated with DAPI for 10 min at room temperature. The antibodies used included Dystrophin, embryonic MyHC (eMyHC), MyoG, and a secondary antibody. Antibody details are presented in Supplementary Materials, Table S4.

Single myofiber isolation and culture

Individual muscle fibers were isolated from extensor digitorum longus (16) muscle of mice as described previously (48). Briefly, EDL muscles were isolated and digested with 2 mg/ml collagenase I (C0130) in DMEM for 1 h at 37°C. Digestion was stopped by carefully transferring the EDL muscles. Add 6 ml of DMEM containing 10% horse serum into a preheated petri dish (10 cm); at that point, the muscles start to contract. Then, gently rinse muscles with a P200 micropipette to release individual muscle fibers. The released individual muscle fibers were transferred and cultured in DMEM in a matrix gel-coated Petri dish (10 cm) supplemented with 20% FBS, 4 ng/ml basic fibroblast growth factor and 1% penicillin–streptomycin at 37°C and 5% CO_2.

Muscle injury and regeneration

Muscle injury was performed as reported previously (49). Briefly, we injected 50 μl phosphate-buffered saline containing 10 mM cardiotoxin (CTX) (Sigma, USA) into the TA muscles of 8-week-old male mice and injected 100 μg EdU (Thermo Fisher Scientific, USA) intraperitoneally 4 h before harvesting muscles.

RNA immunoprecipitation (RIP) assay

RNA immunoprecipitation was performed using the Magna RIP RNA-Binding Protein Immunoprecipitation Kit (Millipore, USA) according to the manufacturer's instructions. The p300, Smarca5 and H3K27ac antibodies were used for RIP. Co-precipitated RNA was detected using reverse transcription PCR (RT-PCR) or qRT-PCR. The qRT-PCR data was presented as a percentage of the input, as described previously (50).

Biotin-labelled RNA pulldown and mass spectrometry

Biotin-labelled RNA pulldown was performed according to a previously published method (26). The proteins pulled down by *lncMREF* were used for Western blotting. For mass spectrometry, the proteins pulled down by *lncMREF* were separated using a 10% sodium dodecyl sulfate polyacrylamide gel electrophoresis (SDS-PAGE) gel and then subjected to the silver staining. The differentially expressed bands were cut out and used for mass spectrometry (Novogene, China). The proteins whose sense strand binding abundance is 5 times or more than that of antisense strand and *q*-value <0.01 were considered to be *lncMREF* binding proteins.

RNA-seq and data analyses

For library construction, we used a protocol as described before (43). The purified library products were evaluated using a Bioanalyzer (Agilent) and SYBR qPCR and sequenced on an Illumina Hi-seq2000 sequencer (pair-end with 50 bp). Raw reads were filtered by Trim Galore (v 0.6.6) to remove low quality reads and adaptor sequences. Paired-end reads were aligned to mm10 genome with Hisat2 (v2.2.1). FeatureCounts (v 2.0.1) was used to quantify the differences in gene expression to obtain the raw counts data. Then, DEseq2 (v 1.28.1) was used to standardize the raw counts and analyze the differences. Genes with |fold change| > 1.5 and P_{adj} < 0.05 were considered as significantly differentially expressed genes. All primers used in qRT-PCR are presented in Supplementary Materials, Table S1.

Chromatin immunoprecipitation (ChIP)-Seq and ChIP-qPCR

The ChIP experiments were performed as described previously (51). Briefly, lysates were generated from 4×10^6

cells. Each lysate was immunoprecipitated with 5 μg of anti-p300 (ab8580 from Abcam), 5 μg of anti-histone H3 lysine 27 acetylated (H3K27ac, ab4729 from Abcam) and the corresponding control IgG, respectively. Antibodies were pre-conjugated to 25 μl of A/G protein-coupled paramagnetic beads (ThermoFisher) in 0.5% PBS/BSA at 4°C. Beads were then added to the lysate and allowed to undergo overnight incubation. Beads were washed six times with modified RIPA buffer (50 mM HEPES [pH 7.6], 500 mM LiCl, 1 mM EDTA, 1% NP-40 and 0.7% sodium deoxycholate) and once with TE containing 50 mM NaCl. DNA was eluted in solution TE containing 2% SDS and cross-linking was incubated at 65°C for 2 h in reverse. DNA was then purified by Qiaquick columns (Qiagen). The DNA was used for library construction or qPCR analysis by using specific primers (Supplementary Table S1). Libraries were constructed using the ChIP Elution Kit and the DNA Smart ChIP Seq Kit from a low input DNA template (Illumina) sequencing library preparation with 75nt paired ends. Raw reads were pocessed by Trimomatic (v 0.39) to remove low quality reads and adaptor sequences. The resulting trimmed reads were aligned to mm10 by Bowtie2-align-s (v 2.4.4). Duplicate reads were marked and removed by Picard MarkDuplicates (http://broadinstitute.github.io/picard/). The reads whose mapping quality >30 were used for further analysis. The Bam files were converted to BigWig profiles by using Deeptools (v 3.5.1) for visualization in the Integrative Genomics Viewer (v 2.9.2). Detected by Macs2 (v 2.2.7.1) with the cutoff *P*-value 5-e2, the peaks were analyzed for differences by R package Diffbind (v 2.16.2). Peaks with the *P*-value < 0.05 and |fold change| > 2 were considered as significantly differential peaks. Bioconductor package ChIPseeker (v 1.24.0) and TxDb.Mmusculus.UCSC.mm10.knownGene (v 3.10.0) were used to annotate the differential peaks. All primers used in qRT-PCR are presented in Supplementary Materials, Table S1.

RNA electrophoretic mobility shift assay (EMSA)

RNA EMSA was performed according to a previously published method (52). Biotin-labeled RNA probes were generated by *in vitro* transcription using cDNA containing T7 promoter and the *lncMREF* fragment RNA were purchased from Genephamra (Shanghai, China). For the RNA EMSA assay, recombinant Flag-Smarca5 or p300, 100 ng/ml tRNA, and 1 μg of biotin-labeled RNA probe were mixed in binding buffer (10 mM Tris–Cl, pH 7.5, 25 mM KCl, 10 mM MgCl₂, 1 mM DTT) for 30 min at 25°C and then separated in 6% native poly acrylamide gel. RNA–protein complexes were blotted with HRP-conjugated streptavidin and the results were visualized by autoradiography.

Single-cell RNA sequencing data analyses

The single-cell sequencing data of basal condition and 3-day post CTX injury was from GEO database (GSE129057) (53) and raw counts were downloaded for further analysis. Bioinformatics analyses were performed in R (v. 4.0.2) and quality control was performed using the package Seurat (v. 4.0.2). The variance stabilizing transformation (VST) method and canonical correlation analysis (CCA) method were used to identify top 2000 variable genes and integrate data in Seurat, respectively. The Uniform manifold approximation and progression (UMAP) plot was used to visualize clustering data. Genes used to define different cell identities in the single-cell RNA sequencing were determined according to the published literature (53).

Generation of *Smarca5* knockout C2C12 cells using CRISPR/Cas9

Smarca5 knockout C2C12 cells were generated by CRISPR/Cas9 using the pSpCas9(BB)-2A-GFP (PX458) plasmid. The single guide RNAs (sgRNAs) (5′-GCGCGCCTTCCAAGCCCTCGG-3′) were designed using an online CRISPR design tool (http://tools.geneome-engineering.org) to cause frame shift mutation in the protein-coding regions. The primers (F: 5′-CACCGCGCGCCTTCCAAGCCCTCGG-3′; R: 5′-AAACCCGAGGGCTTGGAAGGCGCGC-3′) were designed with an added *Bbs*I (ThermoScientific, FD1014) restriction site and an extra G/C for increased hU6 promoter efficiency, annealed and ligated to BbsI-linearized pSpCas9(BB)-2A-GFP (PX458) plasmid using the T4-ligase (ThermoScientific, EL0011). A total of 1.5×10^5 C2C12 cells were transfected with 7 μg of plasmid with Lipofectamine 2000 reagent and then the cells were FACS-isolated. Successful knockout C2C12 cells were validated through PCR amplification with the specific primers (F: 5′-AGGTCTCACTCCTCCGGC-3′; R: 5′-AAATACTTCCTCCATCTCGGTG-3′) and sequencing.

Protein purification and glutathione-S-transferase (GST) pulldown

The pET-GST-Smarca5, pET-GST-Smarca5-Mut, pET-GST-p300, pET-GST-p300-Mut, or empty pET-GST were transformed into Escherichia coli (Thermo, San Jose, CA, USA), separately. Bacteria were grown to an OD600 of 0.8–1.0 and then induced with 0.5 mM IPTG (Sigma) for 2 h at 37°C in a shaking incubator. Smarca5-GST protein and p300-GST protein were purified using the GST spin purification kit (Beyotime Biotechnology, P2262) according to the manufacturer's instruction. Briefly, the bacterial solution was collected and washed three times with PBS. Lysozyme was added to a final concentration of 1 mg/ml, and placed on ice for 30 min, then centrifuged at 4°C for 10 min. The supernatant was purified using the Beyo-Gold™ GST-tag Purification Resin. Finally, the protein was eluted from the column. The purified protein was stained with Coomassie brilliant blue, and the staining method was in accordance with the instructions of the kit (Beyotime Biotechnology, P0017). Smarca5-GST protein and p300-GST protein were incubated with total proteins extracted from C2C12 cells and rotated overnight at 4°C in reaction buffer (50 mM Tris (pH 7.5), 0.1 mM Ethylenediaminetetraacetic acid, 1% Triton X-100, 10% glycerol, 1 mM phenylmethylsulfonyl fluoride, and 1 mM DTT). Then, Glutathione agarose beads (Thermo) were added and allowed to incubate for 2 h at 4°C and then washed with

the washing buffer. Samples were eluted by incubation with Laemmli sample buffer (Bio-rad, CA, USA) and denatured at 98°C for 10 min. Samples were tested by Western blotting and the immunoblotting was performed against FLAG (1:1000, Sigma) to detect FLAG-tagged protein and against GST to detect GST protein as a loading control.

Assay for transposase accessible chromatin with high-throughput sequencing (ATAC-seq) and bioinformatics analyses

ATAC-seq was performed using the TruePrep DNA Library Prep Kit V2 for Illumina (Nanjing Vazyme, China) according to the manufacturer's instructions. Briefly, cell pellets were resuspended in lysis buffer, pelleted and tagmented by using the enzyme and buffer provided in the TruePrep DNA Library Prep Kit V2 for Illumina. Trimomatic (v. 0.39) was used for raw reads to remove low quality reads and adaptor sequences. The resulting trimmed reads were aligned to mm10 by Bwa-mem (v. 0.7.17). Duplicate reads were marked and removed by Picard MarkDuplicates (v. 2.25.6). The reads whose mapping quality >20 were used for further analysis. The reads that were aligned to mitochondria were removed by Samtools (v. 1.7) and then converted to BigWig profiles by Deeptools (v. 3.5.1) for visualization in the Integrative Genomics Viewer (v. 2.9.2). Peaks were identified by using the Macs2 (v. 2.2.7.1) with cutoff P-value 5-e2 and nomodel option. R package Diffbind (v. 2.16.2) was used to detect significantly differential peaks (P-value < 0.05 and |fold change| > 1.5). Bioconductor package ChIPseeker (v. 1.24.0) and TxDb.Mmusculus.UCSC.mm10.knownGene (v. 3.10.0) were used to annotate the differential peaks.

HOMER analyses

HOMER analyses were conducted by using the software homer (v. 4.11) findmotifsgenome.pl, and the code is: 'findMotifsGenome.pl atac_homer.bed mm10 atac_homer_motifDir -len 8,10,12', and the remaining parameters including the setting of foreground and background sequence, are all default parameters. TF Motif library comes from Homer's database ('data/knownTFs/known.motifs').

Chromatin isolation by RNA purification (ChIRP)-qRT-PCR

ChIRP was conducted as previously described (54). Briefly, C2C12 cells were harvested and cross-linked with 1% glutaraldehyde. Cells were sonicated at 4°C for 3 h to shear the DNAs to 100–500 bp. Pooled odd and even probes were hybridized with sonicated chromatins and then pulled down using C-1 streptavidin beads (65001; Invitrogen). The pulled down RNAs and DNAs were isolated. The isolated RNAs were used to perform qPCR to check the pulldown efficiency. The DNAs were used for qPCR analysis using specific primers. All primers used in qPCR are presented in Supplementary Materials, Table S1.

Statistical analyses

All differences among groups were analyzed using unpaired or paired Student's *t*-test. $P < 0.05$ was considered to be statistically significant; significance is denoted as *$P < 0.05$ and **$P < 0.01$. All data are presented as mean $\pm$ standard deviation.

RESULTS

lncMREF is mainly expressed in differentiated skeletal muscle satellite cells and promotes myogenic differentiation

Our previous microarray results showed that lncRNA *AK017263* was upregulated by MyoD; qRT-PCR results also confirmed that overexpression of MyoD significantly increased the expression level of *AK017263*, while knockdown of MyoD significantly decreased its expression (55). We named *AK017263* as l̲ncRNA m̲uscle r̲egeneration e̲nhancement f̲actor (*lncMREF*) according to its function in promoting muscle regeneration via subsequent analysis. *lncMREF* was mapped in the intergenic region of *Eif4g2* (eukaryotic translation initiation Factor 4 gamma 2) and *Galnt18* (polypeptide N-acetylgalactosaminyltransferase 18) on mouse chromosome 7. We used RACE to identify *lncMREF* as a lncRNA with the full length of 1144 bp (Supplementary Figure S1A), which was submitted to GenBank (MW39524). *In vitro* translation experiments indicated that *lncMREF* is a noncoding RNA (Figure 1A). The qRT–PCR results showed that *lncMREF* was mainly expressed in muscle tissues, such as in the *longissimus dorsi* muscle, leg muscle, tongue and heart (Figure 1B). In addition, the expression of *lncMREF* increased and then decreased during embryonic and postnatal muscle development, which was consistent with the expression pattern during C2C12 cell differentiation (Supplementary Figure S1B-E). Cell fractionation experiments demonstrated that *lncMREF* was mainly distributed in the nuclei of differentiated myoblasts (Figure 1C). Bioinformatics analysis of published ChIP-seq data (GSE56131) showed that significant binding peaks of MyoD were detected in the promoter region of *lncMREF* (Figure 1D). The motifs of MyoD from the JASPAR database (http://jaspar.genereg.net/) were also detected in the binding region (Supplementary Figure S1F). Mouse skeletal muscle satellite cells were isolated to detect the expression of *lncMREF* in proliferating and activated satellite cells. Pax7 (skeletal muscle satellite cell marker) immunofluorescence staining in the isolated and cultured cells showed that Pax7 positive (Pax7$^+$) cells accounted for 99.32% of total cells, indicating that the isolated cells were satellite cells (Supplementary Figure S1G). Then, immunofluorescence staining for Pax7, MyoD and FISH for *lncMREF* in mouse skeletal muscle satellite cells showed that the percentage of MyoD$^+$/Pax7$^+$/*lncMREF*$^+$ and MyoD$^-$/Pax7$^+$/*lncMREF*$^+$ satellite cells was 84.38% and 15.62%, respectively, suggesting *lncMREF* was mainly expressed in the activated muscle satellite cells (Figure 1E). In addition, we compared the expression levels of *lncMREF* in FISCs, ASCs and DSCs by analyzing the published RNA-seq data of different stages of satellite cells (GSE133955) (41) and qRT-PCR verification. The results showed that the expression level of *lncMREF* was upregu-
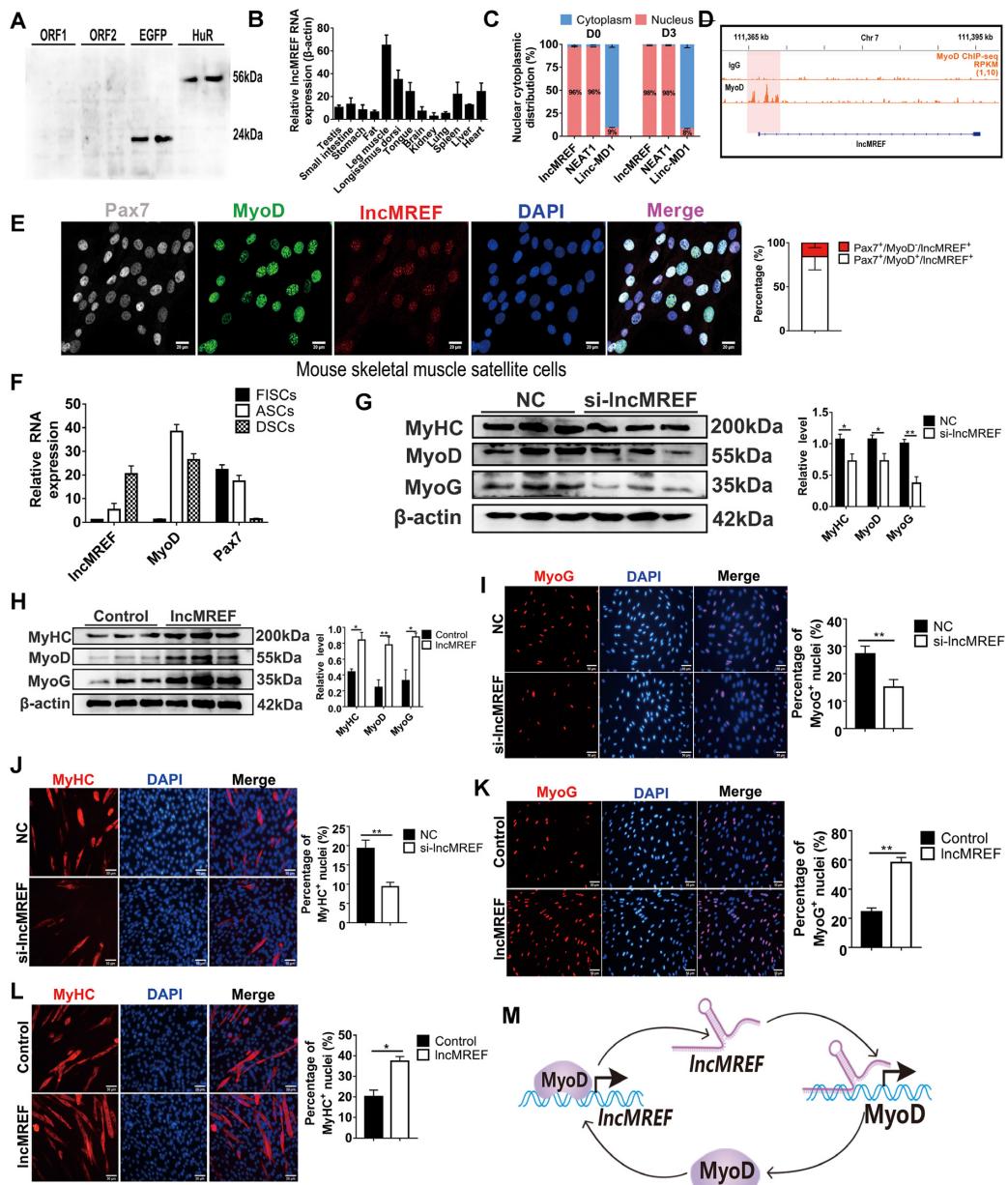
Figure 1. *lncMREF* is mainly expressed in differentiated skeletal muscle satellite cells and promotes myogenic differentiation. (**A**) An *in vitro* translation experiment was performed to determine that *lncMREF* is a noncoding RNA in C2C12 cells. ORF1 and ORF2 represent the two open reading frames in the *lncMREF* sequence, respectively. HuR served as the coding mRNA control. (**B**) qRT-PCR results showed that *lncMREF* was mainly expressed in muscle tissues including *longissimus dorsi*, leg muscle, heart and tongue when *β-actin* was used as the reference gene. (**C**) The distribution of *lncMREF* in the cytoplasm and nuclei of proliferating C2C12 cells (D0) and C2C12 cells differentiated for 3 days (D3) was determined by qRT-PCR. *NEAT1* is a known nuclear lncRNA, and *Linc-MD1* is a cytoplasmic lncRNA. (**D**) Bioinformatic analysis of published ChIP-seq data (GSE56131) showed that the binding peaks of MyoD were detected in the promoter region of *lncMREF*. (**E**) Representative photographs of immunofluorescence staining for Pax7, MyoD and FISH for *lncMREF* in mouse skeletal muscle satellite cells. Quantification of three independent experiments showed that percentage of MyoD$^+$/Pax7$^+$/*lncMREF*$^+$ and MyoD$^-$/Pax7$^+$/*lncMREF*$^+$ satellite cells was 84.38% and 15.62%, respectively. 200 cells were analyzed in an independent experiment. (**F**) qRT-PCR results of *lncMREF* in freshly isolated satellite cells (FISCs), activated satellite cells (ASCs), and differentiated satellite cells (DSCs) showed *lncMREF* expression was significantly unregulated upon satellite cell differentiation. *Pax7* is a specific marker of muscle satellite cells, while *MyoD* is a marker of activation and differentiation of muscle satellite cells. *Pax7* and *MyoD* were used as positive control. The relative RNA levels were normalized to *β-actin*. Data standardization for each gene was based on the lowest level of gene expression in different cell population. (**G, H**) Western blotting results showed that *lncMREF* knockdown significantly decreased the mRNA and protein expression levels of *MyoD*, *MyoG* and *MyHC* genes (G), while *lncMREF* overexpression significantly increased the mRNA and protein expression levels of *MyoD*, *MyoG* and *MyHC* genes (H). (**I–L**) Representative images of immunofluorescence staining for MyoG (I, K) and MyHC (J, L) in differentiated C2C12 myoblasts and quantification showed that *lncMREF* knockdown inhibited myoblast differentiation, while *lncMREF* overexpression promoted myoblast differentiation. Scale bars, 50 μm. (**M**) The diagram of positive feedback loop between *lncMREF* and MyoD: *lncMREF* expression is directly upregulated by MyoD; the upregulation of *lncMREF* further promotes the expression of *MyoD* through unknown mechanisms. A scrambled siRNA was used as a negative control (NC) in gene knockdown experiments, and the empty pcDNA3.1 vector was used as a negative control (Control) in gene overexpression experiments. The relative RNA and protein levels are normalized to those of the control β-actin. The data represent the means ± SD of three independent experiments; $^*P < 0.05$, $^{**}P < 0.01$.

lated upon satellite cell activation and differentiation (Figure 1F and Supplementary Figure S1H and I), indicating that *lncMREF* may play an important role in the differentiation of skeletal muscle satellite cells. To explore the roles of *lncMREF* in myogenesis, we used loss- or gain-of-function experiments to investigate the effects of *lncMREF* on myoblast differentiation in C2C12 myoblasts. In order to detect the proportion of cells overexpressing lncRNA in the population, pcDNA3.1-MCS-EGFP was transfected into C2C12 cells. EGFP immunofluorescence staining and quantification showed the average transfection efficiency was 75.46% (Supplementary Figure S1J). The qRT-PCR, Western blotting and immunofluorescence staining results of differentiated C2C12 myoblasts showed that overexpression of *lncMREF* significantly increased myoblast differentiation, as well as the mRNA and protein expression levels of *MyoD*, *MyoG* and *MyHC*, while knockdown of *lncMREF* significantly suppressed their expression (Figure 1G–L and Supplementary Figure S1K and L). To further determine whether *lncMREF* can transdifferentiate fibroblasts into muscle cells, we conducted the ectopic expression of *lncMREF* in porcine fibroblasts and induced cell differentiation for 4 days. The results showed that *lncMREF* did not induce the expression of myogenic genes such as *MyoD*, *MyoG* and *MyHC* (Supplementary Figure S1M and N). Taken together, there is a positive feedback regulation between *lncMREF* and MyoD: *lncMREF* expression is directly upregulated by MyoD; the upregulation of *lncMREF* further promotes the expression of *MyoD* and myogenic differentiation through unknown mechanisms (Figure 1M).

lncMREF enhances satellite cell differentiation and facilitates muscle regeneration

To detect the effects of *lncMREF* on muscle growth and development *in vivo*, we generated *lncMREF* knockout (KO) mice using CRISPR/Cas9-mediated genome editing. An 811-bp genomic region containing most of the *lncMREF* transcript was deleted, and different genotypes were identified by PCR and sequencing (Supplementary Figure S2A). To determine whether partial deletion of *lncMREF* sequence gives rise to a shorter but still stable RNA, three pairs of qRT-PCR primers targeting exon 1, exon 2 and exons 1–2, respectively, were used to detect both alleles in muscle tissue of wild-type (WT), heterozygous and KO mice. qRT-PCR results showed that although the first exon of *lncMREF* could be detected in KO muscles, the expression level of the first exon in KO muscle was less than 10% of that in WT muscles, suggesting that deletion of exon 2 may decrease the stability of the RNA transcribed from exon 1. Moreover, the expression of *lncMREF* decreased by 50% in the heterozygous mice, compared with WT mice (Supplementary Figure S2B). In order to determine whether there are potential enhancers in the deleted DNA region, we analyzed the histone data labeled with enhancers, and found that there was no potential enhancer in the deleted region (Supplementary Figure S2C). *lncMREF* KO mice were healthy and manifested no significant difference in weight or growth rate compared with WT mice (Figure 2A and

Supplementary Figure S2D). Likewise, there was no significant difference in the weights of the gastrocnemius (Gas), tibialis anterior (TA), and quadriceps (Qu) muscles between 2-month-old WT and KO mice regardless of sex (Figure 2B and Supplementary Figure S2E and F). Hematoxylin and eosin (HE) staining results showed no significant difference in muscle fiber cross-sectional areas between *lncMREF* KO mice and WT mice (Supplementary Figure S2G). In order to investigate whether *lncMREF* KO mice show myopathy like symptoms in their lifespan, we also detected the cross-sectional areas of TA muscles of WT and KO mice at 8, 12 and 18 months by HE staining. The results showed that there was no significant difference in muscle growth and atrophy between the KO and WT mice (Supplementary Figure S2H). To examine whether *lncMREF* affects the number of satellite cells, we performed immunofluorescence on muscle tissues and isolated single muscle fibers, separately. There was no significant difference in the total number of satellite cells between WT and KO mice, as demonstrated by the results of Pax7 (a specific marker of muscle satellite cells) and DAPI staining of single myofibers, as well as Pax7 and dystrophin staining of muscle tissues (Supplementary Figure S2I and J). To further investigate the effects of *lncMREF* on muscle growth and development in mice, we injected the lentivirus-mediated overexpression vector of *lncMREF* (LV-lncMREF) and empty control (LV-control) vector intramuscularly into the left and right legs of 1-month-old WT mice, respectively. The EGFP immunofluorescence staining results showed that there was no significant difference in infection efficiency between the LV-control and LV-lncMREF groups (Supplementary Figure S2K). The qRT-PCR results showed that *lncMREF* expression significantly increased after lentivirus infection (Supplementary Figure S2L). Overexpression of *lncMREF* did not affect the weights of the whole legs, TA, Qu, Gas muscles and the mean cross-sectional areas of individual myofibers (Supplementary Figure S2M-P). To verify the roles of *lncMREF* in satellite cell differentiation, we isolated skeletal muscle satellite cells from the leg muscles of WT and KO mice. Consistent with the results of C2C12 cells, knockout of *lncMREF* in muscle satellite cells significantly decreased cell differentiation according to the qRT-PCR, Western blotting, and immunofluorescence staining results (Figure 2C and D and Supplementary Figure S2Q and R). Moreover, MyoG immunofluorescence staining on isolated single myofibers revealed that *lncMREF* knockout significantly decreased the percentage of MyoG positive (MyoG$^+$) cells by 50% (Supplementary Figure S2S). Together, *lncMREF* promotes satellite cell differentiation, although it does not affect normal muscle growth, suggesting that *lncMREF* may play an important role in muscle regeneration.

To confirm the above hypothesis, we performed CTX-induced TA muscle injury experiments on 2-month-old WT and KO mice. In WT mice, the qRT-PCR results showed that the expression level of *lncMREF* was significantly upregulated at the early stage of injury repair, and decreased after 3 days of injury, which was consistent with the expression patterns of *MyoD* (Figure 2E and F). HE staining results showed that compared with WT mice, *lncMREF*
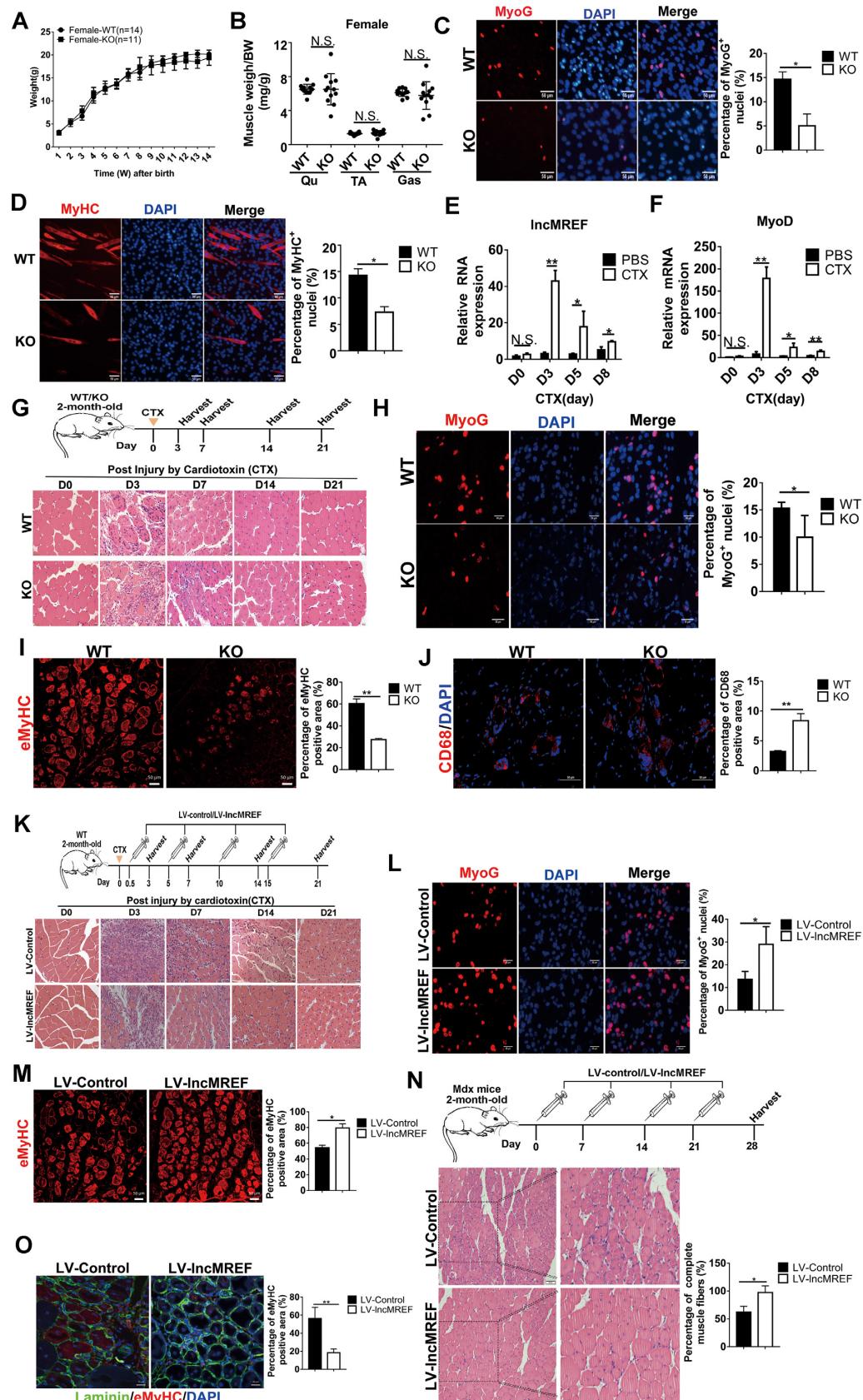
Figure 2. *lncMREF* promotes satellite cell differentiation and facilitates muscle regeneration. (**A**) Growth curves showed that there was no significant difference in growth rate between WT mice (*n* = 14) and *lncMREF* knockout (KO) female mice (*n* = 11). (**B**) There was no significant difference in the

KO mice had a larger number of necrotic myofibers at day 3 (Figure 2G). Immunofluorescence results for MyoG and eMyHC, markers of muscle regeneration, showed that WT mice had a higher number of MyoG-positive (MyoG$^+$) cells and eMyHC positive areas than KO mice at day 3 after CTX injection (Figure 2H and I). Moreover, CD68 (macrophage marker) immunofluorescence staining on TA muscles at 14 days after CTX injection showed that *lncMREF* KO mice had significantly higher percentage of CD68$^+$ areas than WT mice (Figure 2J), indicating *lncMREF* KO muscles had a larger number of inflammatory cells at day 14. The time course of *lncMREF* expression was consistent with phenotypic difference during early regeneration; these results indicated that *lncMREF* KO decreased muscle regeneration at the early stage of muscle injury repair.

To determine whether overexpression of *lncMREF* could accelerate the process of muscle regeneration, we injected the lentivirus-mediated overexpression vector of *lncMREF* (LV-*lncMGPF*) and empty control (LV-control) vector intramuscularly into the left and right legs of 2-month-old KO mice at 12 h after CTX injury, respectively. HE staining results showed that after lentivirus-mediated overexpression of *lncMREF*, the damaged muscle fibers were replaced by regenerated muscle fibers, and repair was almost complete at day 14, while control mice still had many necrotic muscle fibers (Figure 2K). The results of MyoG and eMyHC immunofluorescence staining showed that *lncMREF* overexpression significantly promoted satellite cell differentiation (Figure 2L and M). In addition to acute injury by CTX injection, congenital genetic defects can also cause muscle regeneration due to chronic injury. For example, in a mouse model of Duchenne muscular dystrophy (DMD), extensive muscle degeneration and regeneration occurred as early as 3 weeks old. Repeated degeneration/regeneration cycles result in the loss of muscle satellite cell regeneration and fatty fibrosis in aged DBA/2J-mdx (Mdx) mice (56,57). To examine whether *lncMREF* can affect chronic injury-induced regeneration, we overexpressed *lncMREF* in skeletal muscles of Mdx mice. As expected, the results of HE and immunofluorescence staining for laminin and eMyHC showed that overexpression of *lncMREF* significantly ameliorated muscle damage in Mdx mice (Figure 2N and O). In conclusion, *lncMREF* enhances satellite cell differentiation and facilitates muscle regeneration.

lncMREF regulates myogenic gene expression by recruiting p300/CBP to their promoters

To explore the regulatory mechanism of *lncMREF* in muscle regeneration, we performed RNA-seq in skeletal muscle satellite cells differentiated for 2 days from WT mice and KO mice. In total, 4938 differentially expressed genes (DEGs) (adjusted *P*-value < 0.05, |FC| > 1.5) were identified, of which 2569 genes, including *MyoD* and *Mef2c,* were downregulated, and 2369 genes, including *Trib3* and *Mmp11,* were upregulated (Supplementary Data S1 and Figure 3A). Gene set enrichment analysis (GSEA) showed that *lncMREF* positively regulates muscle cell development and muscle system processes but negatively regulates cytokinesis and axon ensheathment (Figure 3B and Supplementary Figure S3A). To validate the RNA-seq results, we used qRT-PCR to confirm the expression changes of some differentially expressed genes, and the results were consistent with those of RNA-seq (Supplementary Figure S3B). To explore the potential interacting factors of *lncMREF* in the process of muscle regeneration, Metascape software (http://metascape.org/) was used to analyze DEGs (adjusted *P*-value < 0.05, |FC| > 2). The results showed that the predicted transcription factors interacting with *lncMREF* mainly included *MyoD* and p300 (Figure 3C). Due to the positive feedback loop between *MyoD* and *lncMREF* shown in the above results, we focused on p300. Previous studies have reported that p300 plays an important role in muscle development and regeneration by acting as a transcriptional coactivator and mediating H3K27ac (58–62). We speculated that *lncMREF* may regulate target gene expression by interacting with p300. Western blotting results showed that knockdown of *lncMREF* had no significant effect on p300 protein expression in mouse skeletal muscles, but a significant decrease in the overall level of H3K27ac was found after knockdown of *lncMREF* (Figure 3D and E). These results implied that *lncMREF* may recruit p300 to increase H3K27ac levels of target genes. To prove whether there is a physical interaction between *lncMREF* and p300/H3K27ac, we conducted subcellular localization, *lncMREF* RNA pulldown and p300 RIP assays in differentiated mouse skeletal muscle satellite cells. RNA pulldown and RIP assays showed that *lncMREF* can interact with p300 (Figure 3F and G). The RNA FISH for *lncMREF* and immunofluorescence staining for p300 in skeletal
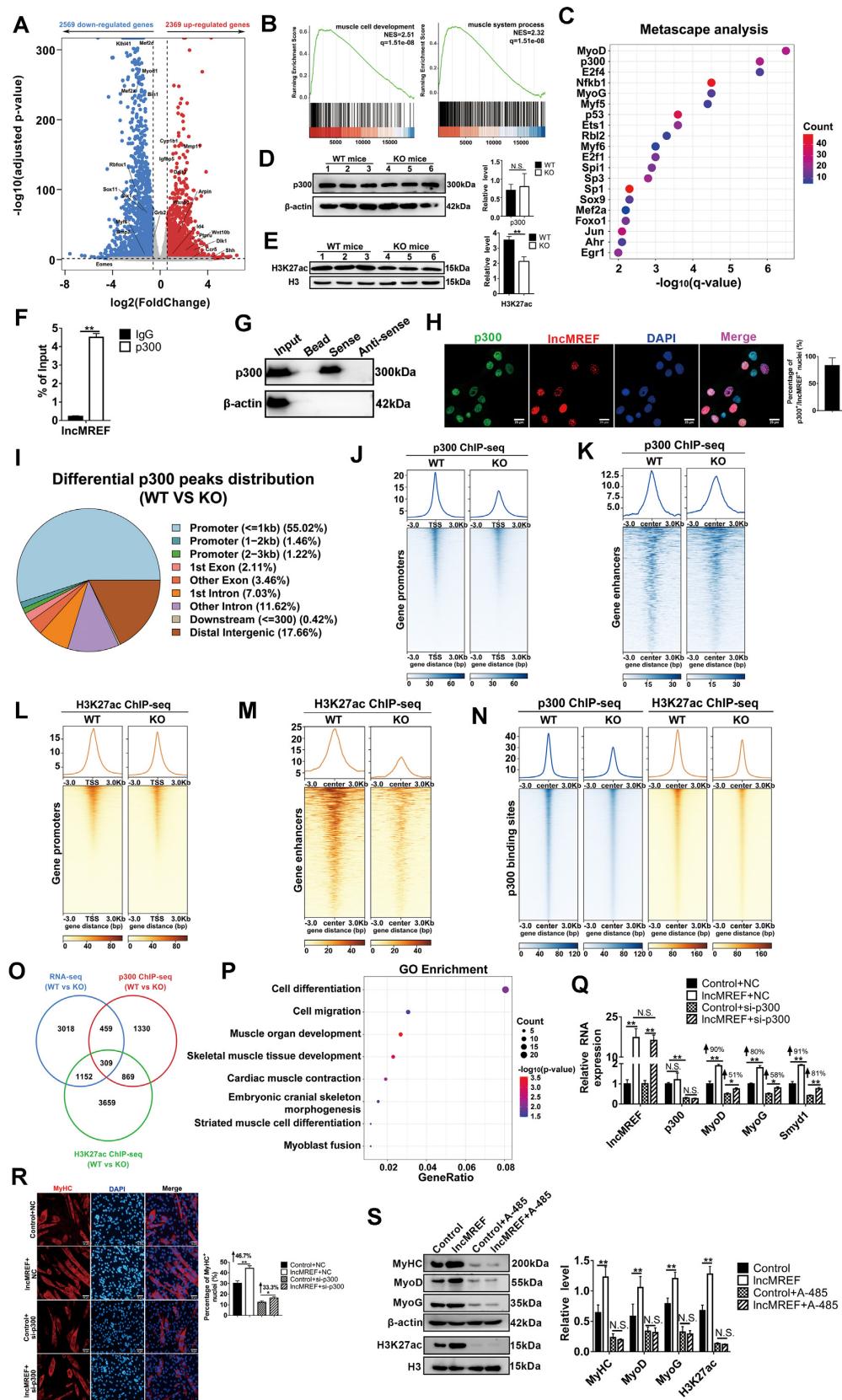
---

weights of the Gas, TA, and Qu muscles between WT mice (*n* = 12) and *lncMREF* KO female mice (*n* = 12). All the data are normalized to the body weights (mg/g). (C, D) Representative images of immunofluorescence staining for MyoG (**C**) and MyHC (**D**) in differentiated muscle satellite cells and quantification of three independent experiments showed that *lncMREF* knockout inhibited myogenic differentiation. Scale bars, 50 μm. (E, F) qRT-PCR results showed that *lncMREF* expression increased significantly at the beginning of the injury and then decrease (**E**), which was consistent with the expression pattern of *MyoD* (**F**). (**G**) Representative photographs of H&E staining for TA muscle at day 0, 3, 7, 14 and 21 after injury showed that WT mice completed muscle damage repair earlier than *lncMREF* KO mice. Scale bars, 20 μm. (H, I) Representative images of immunofluorescence staining for MyoG (**H**) and eMyHC (**I**) of TA muscles at day 3 after injury and quantification showed that lncMREF knockout significantly delayed muscle regeneration. Scale bars, 50 μm. (**J**) Representative images and quantification of three independent experiments of CD68 immunofluorescence staining for TA muscles at day 14 after injury showed that *lncMREF* KO mice had significantly higher percentage of CD68+ macrophages than WT mice. Scale bars, 50 μm. (**K**) Representative photographs of H&E staining for TA muscle at day 0, 3, 7, 14 and 21 after injury showed that *lncMREF* overexpression significantly promoted muscle regeneration. Scale bars, 20 μm. (L, M) Representative images of immunofluorescence staining for MyoG (**L**) and eMyHC (**M**) of TA muscles at day 3 after injury and quantification showed that lncMREF overexpression significantly promoted muscle regeneration. Scale bars, 50 μm. (N, O) Representative images of H&E staining (**N**) and eMyHC/laminin staining (**O**) for TA muscles from 2-month-old Mdx mice injected with lentivirus-mediated *lncMREF* overexpression vector (LV-lncMREF) or control vector (LV-control). The results indicated that lncMREF overexpression significantly ameliorated muscle damage of Mdx mice. Scale bar, 50 μm (N) and 20 μm (O). The lentivirus-mediated empty vector PCDH-CMV-copGFP was used as a negative control (LV-Control) in mouse muscle infection experiments. The relative RNA levels are normalized to those of the control β-actin. The data represent the means ± SD of at least three independent experiments; $^*P < 0.05$, $^{**}P < 0.01$. N.S. indicates statistical non-significance.

Figure 3. *lncMREF* regulates myogenic genes expression by recruiting p300 to their promoters. (**A**) Volcano plot of RNA-seq data showed differentially expressed genes (DEGs) in skeletal muscle satellite cells differentiated for 2 days from WT mice and *lncMREF* KO mice. The DEGs were determined by

muscle satellite cells differentiated for 2 days showed that the percentage of *lncMREF*⁺/p300⁺ and *lncMREF*⁻/p300⁺ cell nuclei accounted for 83.22% and 16.78% of total cell nuclei, respectively, suggesting most of p300 and *lncMREF* are located in the same cell nuclei (Figure 3H).

To further explore how *lncMREF* regulates target gene expression though the p300/H3K27ac pathway, we performed p300 and H3K27ac ChIP-seq in skeletal muscle cells differentiated for 2 days from WT and *lncMREF* KO mice. p300 ChIP-seq results showed that loss of *lncMREF* significantly reduced the enrichment of p300 in 3089 peaks representing 2758 genes, including *MyoD*, *Cdon*, *Myh7* and so on, and increased the enrichment of p300 in 269 peaks representing 209 genes (Supplementary Data S2 and Supplementary Figure S3C). qRT-PCR was used to verify the results of p300 ChIP-seq, and the results were consistent with the ChIP-seq results (Supplementary Figure S3D). The distribution characteristics of differential p300 ChIP-seq peaks showed that 57.7% differential peaks were enriched at gene promoters (Figure 3I). To identify whether p300 binds to the promoters and active enhancers simultaneously, we plotted a heatmap at gene promoters ranging 3kb upstream and downstream of TSS at all genes, as well as at enhancers which were identified in mouse muscle tissue and myoblast from the EnhancerAtlas database (http://www.enhanceratlas.org/downloadv2.php). The results showed that the difference between the mean p300 signals in WT and KO cells at gene promoters was more obvious than that at enhancers (Figure 3J and K). GO enrichment analysis showed that the pathways were mainly associated with the regulation of transcription from RNA polymerase II promoters and skeletal system development, which suggests that *lncMREF* may regulate the differentiation of muscle cells by activating transcription (Supplementary Figure S3E). The H3K27ac ChIP-seq results showed that loss of *lncMREF* significantly reduced

the enrichment of H3K27ac in 11136 peaks representing 4099 genes, including *MyoD*, *Mef2d* and *Myh8*, whereas it increased the enrichment of H3K27ac in 2790 peaks representing 1890 genes (Supplementary Data S3 and Supplementary Figure S3F). qRT-PCR results of H3K27ac ChIP were consistent with the ChIP-seq results (Supplementary Figure S3G). Compared with genomic distribution of p300 differential binding sites, H3K27ac differential binding peaks between WT and KO satellite cells were more evenly distributed in the gene body and intergenic regions (Supplementary Figure S3H). Moreover, we plotted the heatmap of H3K27ac ChIP-seq at gene promoters and enhancers. The results indicated that the difference between the mean H3K27ac signals in WT and KO cells at enhancers was more remarkable than that at gene promoters, suggesting *lncMREF* mainly affects H3K27ac binding capacities to enhancers (Figure 3L and M). GO enrichment analysis showed that the pathways were mainly associated with the regulation of transcription in cell differentiation, chromatin remodeling and histone H3 acetylation (Supplementary Figure S3I). To explore the model of *lncMREF* regulation through p300/H3K27ac pathway, the heatmap of the signals of H3k27ac ChIP-seq in the p300 binding region was further plotted, and the results showed that the p300 decrease coincides with a decrease in H3K27ac signals (Figure 3N). Furthermore, we integrated the RNA-seq data of *lncMREF*, p300 and H3K27ac ChIP-seq data, and found that there were 309 common regulated genes after *lncMREF* KO, including *MyoD*, *Cdon*, and *Myh7* (Figure 3O). GO enrichment analysis revealed that 309 common regulated genes were mainly involved in cell differentiation and muscle organ development (Figure 3P and Supplementary Figure S3J). Moreover, we co-transfected a *lncMREF* overexpression vector and p300 siRNAs in mouse skeletal muscle satellite cells to confirm that *lncMREF*-mediated gene expression is dependent on p300. The qRT-PCR and West-

adjusting *P*-value <0.05 and absolute FC > 1.5. A total of 4938 DEGs were identified, of which 2569 genes were downregulated and 2369 genes were upregulated. (**B**) GSEA plot of muscle cell development(left)- and muscle system process(right)-related genes in skeletal muscle satellite cells differentiated for 2 days from WT mice and *lncMREF* KO mice. (**C**) Metascape databases were used to predict the transcription factors interacting with *lncMREF*. (D, E) Western blotting results showed that *lncMREF* knockout had no significant effect on the protein expression of p300 in mouse skeletal muscles (**D**), but significantly decreased the protein level of H3K27ac (**E**). Lanes 1–3 corresponded to the WT individual 1–3, and lane 4–6 represented the KO individual 4–6, respectively. (F, G). The results of RNA pulldown (**F**) and RIP (**G**) assays in C2C12 myoblasts showed that p300 could bind to *lncMREF*. Input and IgG were used as positive and negative controls, respectively. β-actin and GAPDH that could not bind to *lncMREF* were used as negative control proteins. There was no RNA in bead group, and the sense and anti-sense groups represented the addition of *lncMREF* sense and anti-sense RNA, respectively. (**H**) Representative photographs of *lncMREF* RNA FISH and immunofluorescence staining for p300 showed that 83.22% of *lncMREF* and p300 were located in the same cell nuclei of skeletal muscle satellite cells differentiated for 2 days. (**I**) Pie charts showing the distribution of differential p300 peaks between WT and KO satellite cells across the genome. Different colors represent different genomic regions. The differential p300 peaks were distributed at gene promoter (57.7%), exon (5.57%), intron (18.65%), downstream (0.42%) and distal intergenic regions (17.66%). Cells from five mice WT and KO mice were analyzed in ChIP-seq experiments, respectively. The number of cells used in each ChIP experimental group was 5×10^4. (J, K) Heatmap of p300 ChIP-seq signals at gene promoters (**J**) and enhancers (**K**) gene between WT and *lncMREF* KO satellite cells. (L, M) Heatmap of H3K27ac ChIP-seq signals at gene promoters (**L**) and enhancers (**M**) between WT and *lncMREF* KO satellite cells. Cells from five mice WT and KO mice were analyzed in ChIP-seq experiments, respectively. The number of cells used in each ChIP experimental group was 5×10^4. (**N**) Heatmap of the signals of p300 ChIP-seq (blue) and H3K27ac ChIP-seq (orange) at the p300 binding sites between WT and KO cells showing that the p300 decrease coincides with a decrease in H3K27ac signals. Enrichment signal was plotted relative to peak center ± 3 kb. Each row represents a 6kb genomic region flanking the p300 binding sites. Top panels display the average signal within each category in the same color. (**O**) Venn diagram showing the number of common differentially regulated genes among RNA-seq, p300 ChIP-seq and H3K27ac ChIP-seq. (**P**) GO enrichment dot plot of 309 common regulated genes among RNA-seq, p300 and H3K27ac ChIP-seq. (Q, R) qRT-PCR results (**Q**) and representative photographs of MyHC immunofluorescence staining (**R**) showed that *p300* knockdown attenuated the promoting effects of *lncMREF* on the expression of *MyoD*, *MyoG* and *Smyd1*, as well as myogenic differentiation. (**S**) Western blotting results in C2C12 myoblasts differentiated for 4 days showed that the addition of A-485 abolished the promoting effects of *lncMREF* on the expression of myogenic genes such as *MyoD*, *MyoG* and *MyHC*. A scrambled siRNA was used as a negative control (NC) in gene knockdown experiments, and the empty pcDNA3.1 vector was used as a negative control (Control) in gene overexpression experiments. The relative RNA and protein levels are normalized to those of the control β-actin. The data represent the means ± SD of three independent experiments; $^*P < 0.05$, $^{**}P < 0.01$. N.S. indicates statistical non-significance.

ern blotting results indicated that overexpression of *lncM-REF* increased the expression of *MyoD* and *Mef2s*, and *p300* knockdown attenuated *lncMREF* activity (Figure 3Q and Supplementary Figure S3K). Similarly, the results of MyHC immunofluorescence indicated that knockdown of *p300* attenuated the promotion effect of *lncMREF* on myoblast differentiation (Figure 3R). However, overexpression of *lncMREF* in *p300* knockdown cells still promoted the expression of myogenic genes. These phenomena might be caused by the existence of CBP, which may compensate for the function of p300. In order to further confirm this conjecture, we performed *lncMREF* RNA pulldown experiments, and the results showed that *lncMREF* also interacted with CBP (Supplementary Figure S3L). Then, we used A-485, inhibitor of p300/CBP enzyme activity, to treat C2C12 cells, and then conducted *lncMREF* overexpression experiments. The results showed that overexpression of *lncMREF* had no significant effects on the expression of target genes and myogenic differentiation after inhibition of p300/CBP enzyme activity (Figure 3S and Supplementary Figure S3M and N). Altogether, we concluded that *lncMREF* activates the differentiation of satellite cells by increasing p300/CBP and H3K27ac enrichment at the target genomic regions.

Smarca5 is required for the interaction of *lncMREF* with p300 and the function of *lncMREF*

To assess whether p300 directly binds to *lncMREF*, we conducted an RNA EMSA. GST-p300 recombinant protein was expressed in E. coli, purified by GST-tag Protein Purification Kit, and then identified by Coomassie Brilliant Blue staining (Supplementary Figure S4A). The results showed that the purified recombinant GST-p300 did not affect the migration of *lncMREF* RNA probes, suggesting that if an interaction occurs between p300 and *lncMREF*, it possibly requires additional factors (Figure 4A). Therefore, we inferred that this additional factor may have three features: (1) it is expressed at low levels or not expressed in resting satellite cells but highly expressed in activated satellite cells; (2) it can bind to *lncMREF* and p300, respectively; and (3) it can promote myogenic differentiation of satellite cells, which is consistent with the function of *lncMREF*.

To identify this additional factor, we first analyzed publicly available microarray data (GSE45577) showing gene expression changes during the time course of CTX-induced mouse muscle regeneration and identified 2612 upregulated and 1745 downregulated genes (day 3 versus day 0). Then, we performed *lncMREF* RNA pulldown and mass spectrometry to identify the interacting proteins in differentiated C2C12 cells and mouse skeletal muscle satellite cells. We screened the proteins in *lncMREF* pulldown experiments with a *q*-value < 0.01. A total of 122 common interacting factors were identified in C2C12 cells and skeletal muscle satellite cells, of which 26 genes overlapped with upregulated genes (day 3 versus day 0) after injury (Figure 4B). Although p300 was found in our mass spectrometry, its *q*-value was 0.1022, which did not meet the criteria, so it was not shown in the *lncMREF* target protein data. Among these 26 interacting genes, *Smarca5* attracted our attention, as it is reported to be a chromatin remodeling factor involved in chromatin modifications. Firstly, we detected

the expression of *Smarca5* during embryonic and postnatal muscle development. qRT-PCR results showed that the relative expression level of *Smarca5* was very low compared with *MyHC* expression during embryonic and postnatal muscle development (Supplementary Figure S4B). Then, Western blotting and qRT-PCR results confirmed that *Smarca5* expression was significantly upregulated after CTX-induced muscle injury (Supplementary Figure S4C and D). To confirm that the increase in *Smarca5* could come from muscle stem cells, we re-analyzed the published single-cell sequencing data of basal condition and 3-days post CTX injury from GEO database (GSE129057). UMAP plot identified 7 distinct cell types, including activated muscle satellite cells (MuSC), quiescent MuSC, activated endothelial cells (EC), EC, myoblast, smooth muscle cells (SMC) and macrophage (Supplementary Figure S4E and F), which was consistent with the reported results (53). Further analyses of *Smarca5* expression in different cell clusters showed that *Smarca5* was expressed lowly in quiescent MuSC, but significantly upregulated in activated MuSC (Figure 4C). Immunofluorescence staining for Pax7, MyoD and Smarca5 in skeletal muscle satellite cells and quantification showed that the percentage of MyoD$^+$/Pax7$^+$/Smarca5$^+$ and MyoD$^-$/Pax7$^+$/ Smarca5$^+$ satellite cells was 96.44% and 3.56%, respectively, suggesting Smarca5 was mainly expressed in the activated muscle satellite cells (Supplementary Figure S4G). RNA pulldown and RIP assays showed that *lncMREF* and Smarca5 interacted with each other (Figure 4D and E). The RNA EMSA results further confirmed that Flag-Smarca5 could bind to *lncMREF* (Figure 4F). Co-immunoprecipitation (co-IP) results showed that Smarca5 could interact with p300 (Figure 4G). To further explore whether p300 binds to Smacra5, we performed GST pulldown experiments. The Flag-Smarca5 recombinant protein was expressed in eukaryotic cells (293T cells) and purified using the Flag-tag protein purification kit (Beyotime Biotechnology, P2181). Coomassie brilliant blue staining showed that Flag-Smarca5 protein was successfully expressed (Supplementary Figure S4H). The GST pulldown results showed that GST-p300 could bind to Flag-Smarca5 (Figure 4H). In addition, The RNA FISH for *lncMREF* and immunofluorescence staining for p300 and Smarca5 in skeletal muscle satellite cells differentiated for 2 days showed that *lncMREF*$^+$/p300$^+$/Smarca5$^+$ cell nuclei accounted for 81.29% of total cell nuclei, indicating that most of *lncMREF*, p300 and Smarca5 are located in the same cell nuclei (Figure 4I). To verify the function of the *Smarca5* gene in myogenesis, loss- or gain-of-function experiments were performed in C2C12 cells. As expected, overexpression of *Smarca5* promoted the differentiation of C2C12 cells (Figure 4J–M), and knockdown of *Smarca5* inhibited C2C12 cell differentiation (Supplementary Figure S4I–L). Moreover, we constructed *Smarca5* knockout C2C12 cells using CRISPR/Cas9 gene editing techniques. Consistent with the results of Smarca5 knockdown, *Smarca5* knockout significantly reduced the myogenic differentiation of C2C12 cells (Supplementary Figure S4M–P). Taken together, Smarca5 promotes myogenic differentiation and interacts with *lncMREF* and p300.

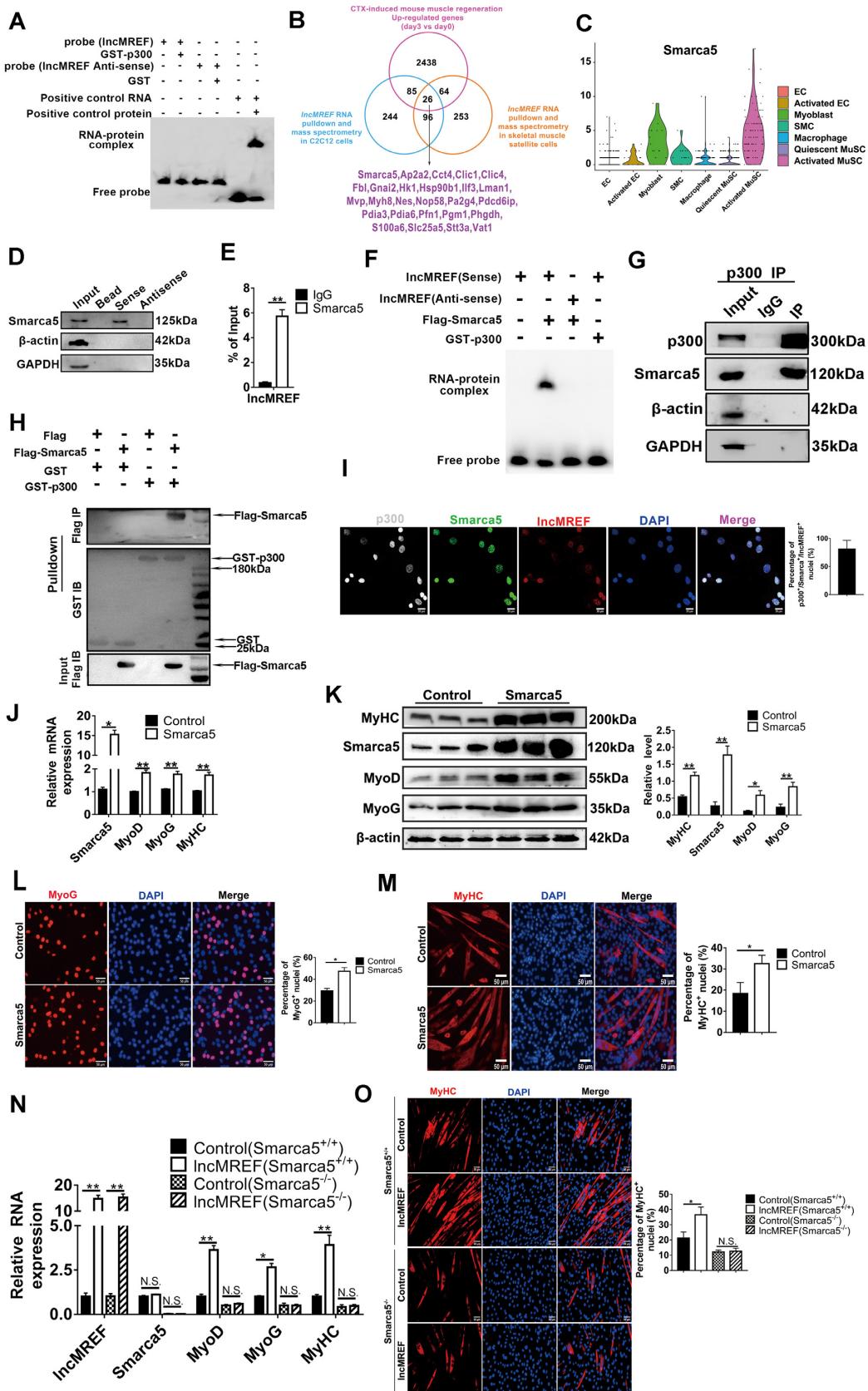To explore the effects of *Smarca5* on *lncMREF*-mediated gene expression, we conducted co-transfection experiments

Figure 4. Smarca5 is required for the interaction of *lncMREF* and p300. (**A**) RNA EMSA results showed that the purified recombinant GST-p300 did not affect the migration of *lncMREF* RNA probes. The negative control RNA was the antisense of *lncMREF*, the negative control protein was the GST protein,

in differentiated mouse skeletal muscle satellite cells. The qRT-PCR, Western blotting and MyHC immunofluorescence staining results indicated that overexpression of *lncMREF* had no significant effects on the expression of myogenic genes such as *MyoD* and *MEF2s*, as well as myogenic differentiation after *Smarca5* knockdown (Supplementary Figure S5A–C). In *Smarca5* knockout cells, no significant effect on cell differentiation caused by overexpression of *lncMREF* was observed (Figure 4N and O). These results suggested that although *Smarca5* was not required for myogenic differentiation, it was still necessary for *lncMREF* to regulate cell differentiation. Meanwhile, we co-transfected the *Smarca5* overexpression vector and *p300* siRNAs into mouse skeletal muscle satellite cells. The qRT-PCR, western blotting and MyHC immunofluorescence staining results indicated that *p300* knockdown significantly attenuated the promoting effect of *Smarca5* on the expression of *MyoD* and *MEF2s* (Supplementary Figure S5D-F). These results revealed that *lncMREF* regulation of myogenic differentiation is dependent on the functions of Smarca5 and p300/CBP.

To identify the core-binding motif of *lncMREF* with Smarca5, we constructed five truncated fragments of *lncMREF* and performed RNA pulldown experiments. The results showed that fragment F5 (213–725 bp) efficiently pulled down Smarca5 (Figure 5A). Two potential binding motifs (motif 1: 5′-533-GUAGACCAGG-542-3′; motif 2: 5′-737-CCUGGUCUAC-746-3′) in fragment F5 were predicted by MEME algorithm analyses. The RNA EMSA results showed that only motif 1 of *lncMREF* could bind to Smarca5 (Figure 5B). *lncMREF* could not bind to Smarca5 when motif 1 was mutated, while *lncMREF* could still bind to Smarca5 after mutating motif 2 (Figure 5C). These results indicated that *lncMREF* combines with Smarca5 via motif 1. To identify the core domain of Smarca5 combined with *lncMREF*, protein expression vectors of different domains of Smarca5 were constructed separately, and RNA EMSA experiments were performed with *lncMREF*. The results showed that *lncMREF* binds to the SLIDE domain of Smarca5 (Figure 5D). To explore the core domain where Smarca5 interacts with p300, we constructed eight different domains of p300 into Flag fusion expression vectors and seven different domains of Smarca5 into Flag fusion expression vectors according to the protein database information (http://www.ebi.ac.uk/interpro/result/InterProScan). The results of IP experiments showed that Smarca5 specifically interacted with p300 through its 482–596 amino acids (AA) domain (Figure 5E), while p300 specifically recognized Smarca5 through its unique 567–647 AA domain (Figure 5F). GST pulldown experiments showed that deletion of these two domains resulted in the failure of the interaction between p300 and Smarca5 (Figure 5G and H), further confirming that the 482–596 AA domain of Smarca5 and 567–647 AA domain of p300 are the core interacting domains. The above results showed that Smarca5 interacts with motif 1 of *lncMREF* via the SLIDE domain and specifically recognizes the 567–647 AA domain of p300 via its 482–596 AA domain.

To investigate the roles of Smarca5 in the interaction between *lncMREF* and p300, we performed p300 RIP experiments in *Smarca5*-overexpressing and *Smarca5*-knockdown cells. Overexpression of *Smarca5* significantly increased the binding capacity of *lncMREF* to p300, while knockdown of *Smarca5* significantly decreased the binding capacity of *lncMREF* to p300 (Figure 5I and J). p300 RIP experiments in *Smarca5* knockout C2C12 cells further confirmed that p300 failed to interact with *lncMREF* in the absence of Smarca5 (Figure 5K). In contrast, the Smarca5 RIP experiment results showed that p300 knockdown or overexpression had no significant effect on the interaction of *lncMREF* with Smarca5 (Figure 5L). In addition, Co-IP experiments indicated that knockout of *lncMREF* significantly reduced the binding of Smarca5 to p300 (Figure 5M). When the binding motif of *lncMREF* with Smarca5 was mutated, *lncMREF* was unable to bind to p300 and Smarca5 (Figure 5N). The qRT-PCR and immunofluorescence staining

---

and the positive control RNA and protein were provided in the EMSA kit (LightShift® Chemiluminescent RNA EMSA Kit, 20158). (**B**) Overlapping analysis among interacting genes from *lncMREF* pulldown and mass spectrometry data in C2C12 cells differentiated for 2 days and skeletal muscle satellite cells differentiated for 2 days, and upregulated genes in muscles (day 3 vs day 0) during CTX-induced muscle regeneration from the published transcriptomic data (GSE45577). The results showed 122 common interacting factors were identified in C2C12 cells and skeletal muscle satellite cells, of which 26 genes overlapped with upregulated genes (day 3 versus day 0) after injury, such as *Smarca5*. (**C**) Violin diagram showing the *Smarca5* gene expression in activated MuSC, quiescent MuSC, activated EC, EC, myoblast, SMC and macrophage from the published transcriptomic data (GSE129057). The X-axis showed the cell clusters, Y-axis indicated the expression level of cell clusters. Each point denoted a single cell. (D, E) The results of RNA pulldown (**D**) and RIP assays (**E**) in C2C12 myoblasts showed that Smarca5 bound to *lncMREF*. Input and IgG were used as positive and negative controls, respectively. β-actin and GAPDH were used as negative control. There was no RNA in bead group, and the sense and anti-sense groups represented the addition of *lncMREF* sense and anti-sense RNA, respectively. (**F**) The RNA EMSA results showed that *lncMREF* could bind to Flag-Smarca5. The *lncMREF* anti-sense RNA and GST-p300 which could not interact with *lncMREF* were used as negative control RNA and protein, respectively. (**G**) The results of Co-IP experiments showed that Smarca5 could interact with p300. Co-IP was performed with p300 antibody in C2C12 cell lysates, and the purified protein complexes were detected by Western blotting. (**H**) The GST pulldown results showed that GST-p300 could interact with Flag-Smarca5. Flag vector or FLAG-Smarca5 was transfected into 293T cells and immunoprecipitated with anti-FLAG-agarose beads followed by eluting with FLAG peptide. GST-p300 or GST protein was incubated with purified FLAG-Smarca5 or FLAG peptide for pulldown assay, and then incubated with FLAG antibody. GST or GST-p300 protein was detected by immunoblotting with anti-GST antibody. Input was used as positive control. (**I**) Representative photographs of *lncMREF* RNA FISH and immunofluorescence staining for p300 and Smarca5 in skeletal muscle satellite cells differentiated for 2 days. Quantification of three independent experiments showed that *lncMREF*+/p300+/Smarca5+ cell nuclei accounted for 81.29% of the total cell nuclei. 200 cells were analyzed in an independent experiment. Scale bars, 20 μm. (J, K) qRT-PCR (**J**) and Western blotting (**K**) results showed that *Smarca5* overexpression significantly increased the mRNA and protein levels of *MyHC*, *MyoG*, and *MyoD*. (L, M) Representative images of immunofluorescence staining for MyoG (**L**) and MyHC (**M**) in differentiated C2C12 myoblasts and quantification showed that *Smarca5* overexpression promoted myoblast differentiation. Scale bars, 50 μm. (N, O) qRT-PCR results (**N**) and representative photographs of MyHC immunofluorescence staining (**O**) showed that *lncMREF* overexpression had no significant effect on myoblast differentiation in *Smarca5* KO C2C12 myoblasts. The empty pcDNA3.1 vector was used as a negative control (Control) in gene overexpression experiments. The relative RNA and protein levels are normalized to those of the control β-actin. The data represent the means ± SD of three independent experiments; *$P < 0.05$, **$P < 0.01$. N.S. indicates statistical non-significance.
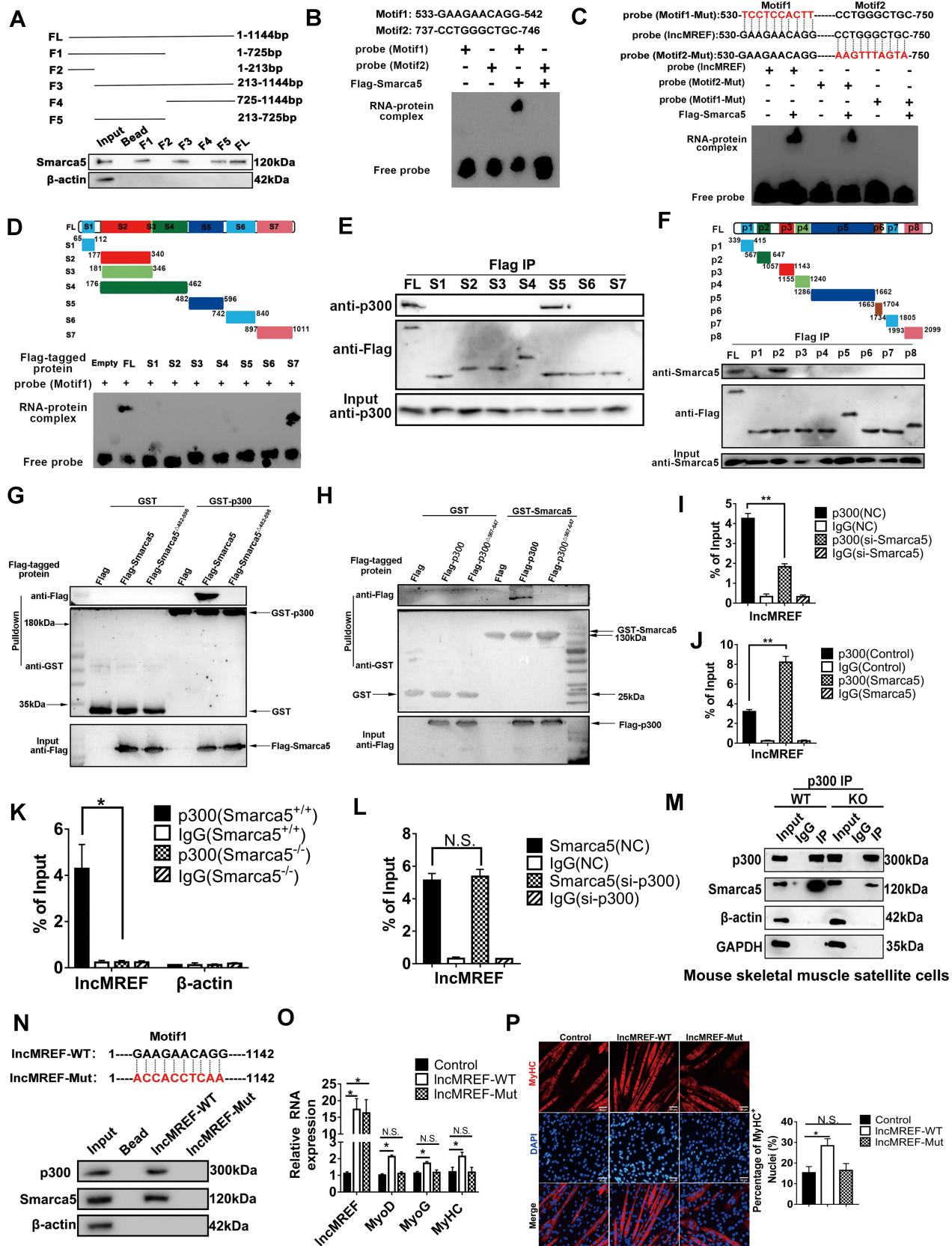
Figure 5. Smarca5 interacts with motif1 of *lncMREF* via SLIDE domain, and specifically recognizes 567–647 AA domain of p300 via its 482–596 AA domains. (**A**) The results of RNA pulldown assays of full-length (FL) and truncated fragments of *lncMREF* showed that FL and F5 (213–725) specifically

results further showed that there was no significant effect of *lncMREF* on myogenic differentiation after mutating the binding motif of *lncMREF* with Smarca5 (Figure 5O and P). In conclusion, Smarca5 is essential for the *lncMREF* regulation of myogenic differentiation, as well as its interaction with p300, and *lncMREF* promotes the interaction between Smarca5 and p300.

lncMREF facilitates p300 genomic binding by upregulating chromatin accessibility of target regulatory regions

Smarca5 acts as a chromatin-remodeling factor and mainly alters the expression of genes by promoting chromatin accessibility (63). p300-catalyzed H2K27ac is often accompanied by changes in chromatin accessibility. We hypothesized that *lncMREF* may affect chromatin accessibility via *Smarca5*. To verify this speculation, we performed an ATAC-seq in skeletal muscle cells differentiated for 2 days from WT and *lncMREF* KO mice. ATAC-seq results showed that loss of *lncMREF* significantly reduced chromatin accessibility in 7368 peaks representing 5537 genes and increased chromatin accessibility in 28 peaks representing 16 genes (Supplementary Data S4). The heatmap showed that knockout of *lncMREF* can significantly reduce chromatin accessibility at gene promoters and enhancers (Figure 6A and B). The distribution characteristics of differential ATAC-seq peaks showed that 43.58% differential peaks were enriched at gene promoters, while 22.41% of the differential peaks were located at distal regulatory regions (Figure 6C). GO enrichment analysis showed that those genes with altered chromatin accessibility were enriched in pathways related to cell differentiation, chromatin modification and remodeling (Figure 6D). Homer motif analysis showed that sequence motifs of myogenic factors, such as MyoD, MyoG and Mef2s, were enriched in the regions with altered chromatin accessibility (Figure 6E). It has been reported that p300 could act as a coactivator of these myogenic transcription factors or histone acetyltransferase to regulate muscle development (58,61). We proposed

that *lncMREF* recruits Smarca5 to enhance the accessible chromatin state, which facilitates p300 and H3K27ac genomic binding to target regulatory regions. Thus, we further detected p300 and H3K27ac signals in the target regions where chromatin accessibility was changed after *lncMREF* deletion. The heatmap of p300 and H3k27ac ChIP-seq signals at the ATAC-seq sites showed that ATAC-seq signal decrease coincided with a decrease in p300 and H3k27ac ChIP-seq signals (Figure 6F). UpSet plot representations were used to comprehensively compare the RNA-seq, p300 ChIP-seq, H3K27ac ChIP-seq and ATAC-seq data (Figure 6G). Of note, 1550 of 2967 genes that were differentially bound by p300 overlapped with genes with chromatin accessibility changes between WT and *lncMREF* knockout cells, suggesting that p300 enrichment at more than half of target genes may be associated with chromatin accessibility. Moreover, 185 common genes were regulated by *lncMREF*, p300, H3K27ac and chromatin accessibility (Figure 6H); these genes included some key myogenic genes, such as *MyoD*, *Cdon* and *Grb2* (Figure 6I–K). To confirm whether *lncMREF* directly regulates these target genes, ChIRP-qRT-PCR was used to detect the binding of *lncMREF* to the promoters of these genes in C2C12 cells differentiated for 2 days. The results showed that *lncMREF* could directly bind to the promoter regions of these genes, indicating that *lncMREF* guides Smarca5 to upregulate chromatin accessibility of target regions (Figure 6L). Taken together, *lncMREF* may recruit Smarca5 to the regulatory regions of its myogenic target regions and enhance chromatin accessibility; the increase in chromatin accessibility leads to an increase in p300/H3K27ac enrichment in target regions, which improves the expression of myogenic genes.

lncMREF is functionally and mechanistically conserved in humans and pigs

Recent studies have shown that many lncRNAs have conserved genomic positions, expression patterns, subcellular distributions, and functional domains among species (64).

---

interacted with Smarca5 in C2C12 myoblasts. β-actin was used as negative control. Input was used as positive control. As shown in the upper image of the Figure, FL represented the full-length of *lncMREF*, F1 (1–725), F2 (1–213), F3 (213–1144), F4 (725–1144) and F5 (213–725) indicated different truncated fragments of *lncMREF*, respectively. (B, C) The RNA EMSA results showed that purified Smarca5 was bound by the motif1 of *lncMRE* (**B**), but the RNA-protein complex cannot form when the motif1 was mutated (**C**). (**D**) The RNA EMSA results showed that *lncMREF* bound to the SLIDE domain of Smarca5 (Smarca5-S7). As shown in the upper image of the Figure, FL represented the full-length of Smarca5, S1 (65–112), S2 (177–340), S3 (181–346), S4 (176–462), S5 (482–596), S6 (742–840) and S7 (897–1011) indicated different truncated fragments of Smarca5, respectively. (E, F) The results of Co-IP experiments showed that Smarca5 specifically interacted with p300 through its 482–596 AA domain (S5) (**E**), and p300 specifically recognized Smarca5 through its unique 567–647 AA domain (p3) (**F**). Co-IP was performed with Flag antibody in C2C12 cell lysates, and the purified protein complexes were detected by Western blotting. As shown in the upper image of the Figure F, FL represented the full-length of p300, p1 (339–415), p2 (567–647), p3 (1057–1143), p4 (1155–1240, p5 (1286–1662), p6 (1663–1704), p7 (1734–1805) and p8 (1993–2099) indicated different truncated fragments of p300, respectively. (**G**) The GST pulldown results showed that p300 could not interact with Smarca5 when the amino acids from 482 to 596 of Smarca5 were deleted. FLAG-tagged Smarca5 and mutant constructs were transfected into 293T cells and purified by using anti-FLAG-agarose beads. GST or GST-p300 fusion protein was incubated with purified FLAG-tagged proteins for pulldown assay. (**H**) The GST pulldown results showed that Smarca5 could not interact with p300 when the amino acids from 567 to 647 of p300 were deleted. FLAG-tagged p300 and mutant constructs were transfected into 293T cells and purified by using anti-FLAG-agarose beads. GST or GST-Smarca5 protein was incubated with purified FLAG-tagged proteins for pulldown assay. (**I, J**) The results of RIP assays results showed that overexpression of *Smarca5* significantly increased the binding capacity of *lncMREF* to p300, while knockdown of *Smarca5* significantly decreased the binding capacity of *lncMREF* to p300. (**K**) The results of RIP assays showed that p300 failed to interact with *lncMREF* after the absence of Smarca5. (**L**) The results of RIP assays showed that p300 knockdown had no significant effect on the interaction of *lncMREF* with Smarca5. (**M**) The results of Co-IP assays showed that knockout of *lncMREF* significantly reduced the interaction of Smarca5 and p300. (**N**) The results of RNA pulldown assays showed that *lncMREF* was unable to bind to p300 and *Smarca5* after mutation of motif1. (O, P) qRT-PCR results (**O**) and representative photographs of MyHC immunofluorescence staining (**P**) showed there was no significant effect of *lncMREF* on myogenic differentiation after mutating the binding motif of *lncMREF* with Smarca5. A scrambled siRNA was used as a negative control (NC) in gene knockdown experiments, and the empty pcDNA3.1 vector was used as a negative control (Control) in gene overexpression experiments. The relative RNA levels are normalized to β-actin. The data are presented as mean ± SD of three independent experiments; $^{*}P < 0.05$, $^{**}P < 0.01$. N.S. indicates statistical non-significance.
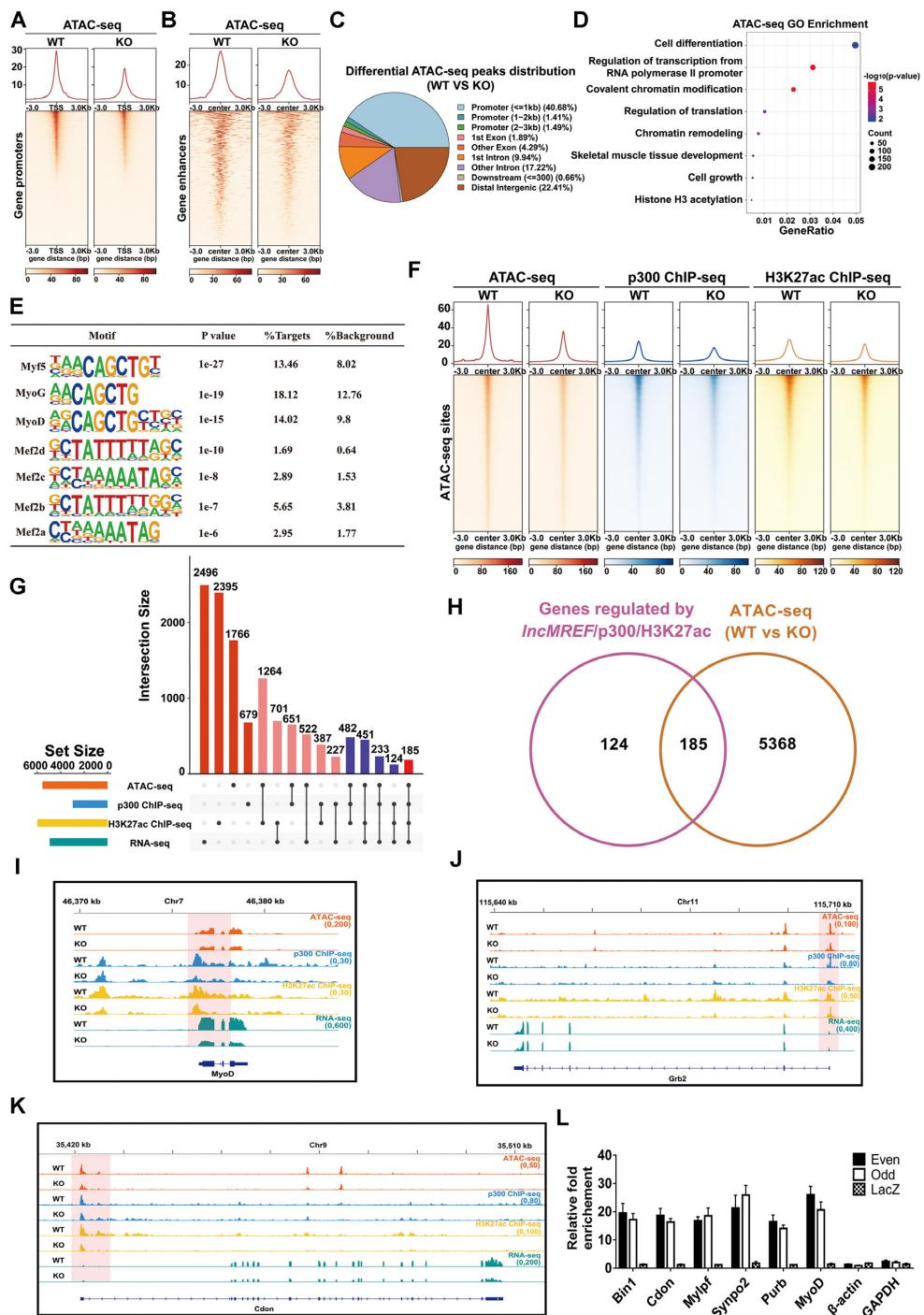
Figure 6. *lncMREF* facilitates p300 genomic binding by upregulating chromatin accessibility of target regulatory regions. (A, B) Heatmap of ATAC-seq signals at promoters (**A**) and gene enhancers (**B**) between WT and *lncMREF* KO skeletal muscle satellite cells. (**C**) Pie charts showing the distribution of differential ATAC-seq peaks between WT and KO satellite cells across the genome. Different colors represent different genomic regions. The differential p300 peaks were distributed at gene promoter (43.58%), exon (6.18%), intron (27.16%), downstream (0.66%) and distal intergenic regions (22.41%). (**D**) GO enrichment dot plot of the genes with differential chromatin accessibility. (**E**) HOMER analysis showed that the binding motifs of myogenic transcription factors were predicted in the target regions where the chromatin accessibility was changed. (**F**) Heatmap of the signals of ATAC-seq (orange), p300 ChIP-seq (blues) and H3K27ac ChIP-seq (yellow) at the genomic loci where ATAC-seq signal changes occur between WT and KO satellite cells. The results showed that there were consistent signal changes among ATAC-seq, p300 and H3K27ac ChIP-seq data at the differential ATAC-seq sites. Enrichment signal was plotted relative to peak center ± 3 kb. Each row represents a 6kb genomic region flanking the ATAC-seq sites. Top panels display the average signal within each category in the same color. (**G**) UpSet plots showing the intersection of multi-omics differentially regulated genes in this study. (**H**) Venn diagram showing that there were 185 common differentially regulated genes by *lncMREF*/p300/H3K27ac and chromatin accessibility. (I–K) Combined profiles of ATAC-seq (orange), ChIP-seq profiles for p300 (blue), H3K27ac (yellow) and RNA-seq (green) for *MyoD* (**I**), *Grb2* (**J**), *Cdon* (**K**). (**L**) ChIRP-qRT-PCR results in C2C12 cells differentiated for 2 days showed that *lncMREF* could directly bind to the promoter regions of *Bin1*, *Cdon*, *Mylpf*, *Synpo2*, *Purb* and *MyoD*.

In the UCSC Genome Browser database, we found that pig lncRNA *MW393523* (termed *plncMREF*) and human lncRNA *MW670463* (termed *hlncMREF*) have conserved genomic positions with mouse *lncMREF*. Both *plncMREF* and *hlncMREF* are transcribed from the genomic region between the *Eif4g2* and *Galnt18* genes (Supplementary Figure S6A). RACE assays showed that *plncMREF* is a transcript 2679 bp in length and *hlncMREF* is a transcript 1833 bp in length (Supplementary Figure S6B and C). *In vitro* translation experiments indicated that *plncMREF* and *hlncMREF* are non-coding RNAs (Supplementary Figure S6D and E). *hlncMREF* and *plncMREF* are gradually upregulated during myogenic progenitor cell differentiation (Supplementary Figure S6F and G). Cell fractionation assays demonstrated that *plncMREF* and *hlncMREF* are mainly distributed in the nuclei of pig myogenic progenitor cells and human skeletal muscle myoblasts, respectively (Figure 7A and B). Interestingly, sequence alignment analysis revealed that *lncMREF* has conserved core-binding motifs of Smarca5 among mice, pigs, and humans (Figure 7C). To investigate the function of *plncMREF* and *hlncMREF* in myogenic differentiation, we overexpressed *plncMREF* and *hlncMREF* in pig skeletal muscle satellite cells and human skeletal muscle myoblasts, respectively. The qRT-PCR, Western blotting and immunofluorescence results showed that overexpression of *plncMREF* and *hlncMREF* significantly promoted the differentiation of pig skeletal muscle satellite cells and human skeletal muscle myoblasts, respectively (Figure 7D and E and Supplementary Figure S6H-M). To further confirm the effects of *plncMREF* and *hlncMREF* on muscle regeneration, we overexpressed *plncMREF* and *hlncMREF* in Mdx mice. HE staining results showed that overexpression of *plncMREF* and *hlncMREF* in Mdx mice significantly alleviated muscle damage (Figure 7F and G). These results indicated that *lncMREFs* are functionally conserved among mice, pigs and humans. To further confirm the conserved mechanisms of *plncMREF* and *hlncMREF*, RNA pulldown was conducted to verify the binding of *plncMREF* and *hlncMREF* to Smarca5 and p300, respectively. Consistent with mouse *lncMREF*, both *plncMREF* and *hlncMREF* interacted with Smarca5 and p300 in pig skeletal muscle satellite cells and human skeletal muscle cells, respectively (Figure 7H and J). RNA EMSA results showed that *plncMREF* and *hlncMREF* could bind to Flag-Smarca5, but not to GST-p300 *in vitro* (Figure 7I and K). RNA pulldown results showed that *plncMREF* and *hlncMREF* could not bind to Smarca5 after mutation of the conserved core-binding motif (Supplementary Figure S6N and O). The qRT-PCR and immunofluorescence staining results further confirmed that there were no significant effects of *plncMREF* or *hlncMREF* on myogenic differentiation after mutating the binding motif of *lncMREF* with Smarca5 (Figure 7L and M). The above results indicated that *lncMREF* is functionally and mechanistically conserved in humans and pigs.

DISCUSSION

Skeletal muscle development and regeneration are complex processes and regulated by a series of transcription factors and important factors. MyoD is a key myogenic tran-

scription factor that can initiate the myogenic differentiation program by transcriptionally regulating the expression of multiple myogenic genes (65,66). It has been reported that MyoD regulates not only the expression of mRNAs and miRNAs but also the expression of lncRNAs, such as *SYISL* (26), *lnc-MD1* (28, and *H19* (67). MyoD performs a pivotal role in muscle differentiation and satellite cell function by divergently regulating lncRNA expression. Firstly, MyoD directly binds to E-box sites at target promoters to activate the expression of the target genes, such as lncRNA *SYISL* (26), *Linc-MD1* (28), *Linc-YY1* (43), *Linc-RAM* (68) and *lncMyoD* (69). These lncRNAs usually promote myogenic differentiation, but several lncRNAs such as *SYISL* inhibit myogenic differentiation. Secondly, MyoD is a 3D genome structure organizer for muscle cell identity and regulates the expression of lncRNAs by changing chromatin structure (70), such as lncRNA *Dum* (31). Thirdly, MyoD possibly regulates the expression of lncRNAs indirectly. For example, MyoD promotes the expression of Myostatin, and then Myostatin inhibits the expression of lncRNA *Malat1*, which in turn inhibits the proliferation of myoblasts (71). In this study, we functionally identified *lncMREF*, which was upregulated by MyoD and in activated skeletal muscle satellite cells, as a novel specific regulator of muscle regeneration. *lncMREF* promotes the differentiation of skeletal muscle satellite cells, but does not transdifferentiate a fibroblast into a muscle cell. Therefore, *lncMREF* rather facilitates myogenic differentiation. Compared with WT mice, *lncMREF* KO mice grew normally without significant muscle phenotype changes and did not show myopathy like symptoms in their lifespan, but showed slower muscle regeneration after muscle injury. This finding further confirmed that lncRNAs function mainly in physiological and pathological diseases. Further functional analyses identified Smarca5 binding motifs within exon 2 as the key functional site of *lncMREF*; loss of this site in KO mice results in the decreased muscle regeneration at the early stage of muscle injury repair. In addition, the function and mechanism of *lncMREF* during myogenesis are conserved among mice, pigs, and humans, which suggests that *lncMREF* may have potential applications for treating muscle diseases, such as muscular dystrophy and Duchenne muscular dystrophy.

LncRNAs regulate gene expression through a variety of mechanisms, including acting as miRNA sponges, regulating mRNA stability and translation, interacting with proteins and DNA/RNA and recruiting epigenetic regulators into target regions (72). For example, *HOTAIR* acts as a modular scaffold for at least two histone-modified complexes (PRC2 and LSD1) and recruits them to target gene promoters (73). *CCAT1-L* interacts with CTCF to upregulate myelocytomatosis oncogene (MYC) proto-oncogene expression through regulation of the chromatin conformation at the MYC locus (74). Here, *lncMREF* could bind to p300/CBP, and knockdown of *lncMREF* reduced the enrichment of p300 in the regulatory region of the genes related to myogenesis, suggesting that *lncMREF* introduces p300/CBP into the regulatory regions of its target genes. p300/CBP is specifically responsible for H3K27ac modification and loosens the chromatin structure to promote transcription initiation (75,76). Several studies have shown that p300 is involved in lncRNA-mediated epigenetic regulation
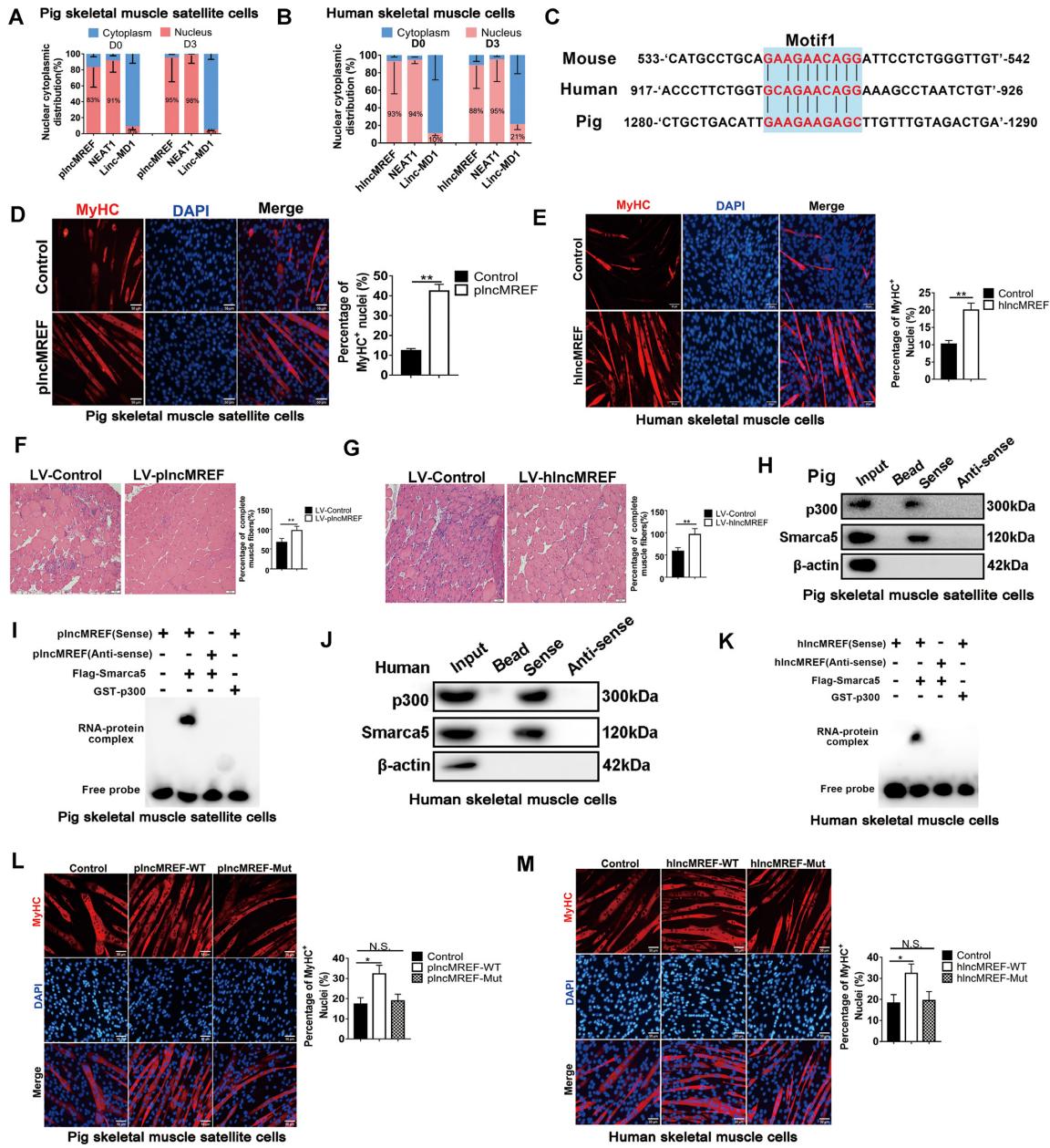
Figure 7. *lncMREF* is functionally and mechanistically conserved in humans and pigs. (**A**) The distribution of *plncMREF* in the cytoplasm and nuclei of proliferating (D0) and differentiated for 3 d (D3) pig skeletal muscle satellite cells was determined by qRT-PCR. *NEAT1* is a known nuclear lncRNA, and *Linc-MD1* is a cytoplasmic RNA. (**B**) The distribution of *hlncMREF* in the cytoplasm and nuclei of proliferating (D0) and differentiated for 3 d (D3) human skeletal muscle cells was determined by qRT-PCR. *NEAT1* is a known nuclear lncRNA, and *Linc-MD1* is a cytoplasmic RNA. (**C**) The conserved core binding motif of *lncMREF* with Smarca5 among mice, pigs and humans was revealed by sequence analysis. (D, E) Representative photographs of MyHC immunofluorescence staining and quantification showed that *plncMREF* (**D**) and *hlncMREF* (**E**) overexpression promoted myoblast differentiation of pig skeletal muscle satellite cells and human skeletal muscle cells, respectively. Scale bar, 50 μm. (F, G) Representative images of H&E staining for TA muscles from 2-month-old Mdx mice injected with lentivirus-mediated *plncMREF* (**F**) or *hlncMREF* (**G**) overexpression vector (LV-plncMREF or LV-hlncMREF) and control vector (LV-control), separately. The results indicated that *plncMREF* (**F**) and *hlncMREF* (**G**) overexpression significantly increased the percentage of complete muscle fibers of Mdx mice, respectively. Scale bar, 50 μm. (H, I) The results of RNA pulldown (**H**) and RNA EMSA (**I**) assays of *plncMREF* showed that *plncMREF* could interact with Smarca5 and p300 in pig skeletal muscle satellite cells, but could not bind to GST-p300 *in vitro*. Input was used as a positive control. There was no RNA in bead group, and the sense and anti-sense groups represented the addition of *plncMREF* sense and anti-sense RNA, respectively. (J, K) The results of RNA pulldown (**J**) and RNA EMSA (**K**) assays of *hlncMREF* showed that *hlncMREF* could interact with Smarca5 and p300 in human skeletal muscle cells, but could not bind to GST-p300 *in vitro*. Input was used as a positive control. There was no RNA in bead group, and the sense and anti-sense groups represented the addition of *hlncMREF* sense and anti-sense RNA, respectively. (L, M) Representative photographs of MyHC immunofluorescence staining and quantification showed that there was no significant effect of *plncMREF* (**L**) or *hlncMREF* (**M**) on myogenic differentiation after mutating the binding motif of *lncMREF* with Smarca5. The empty pcDNA3.1 vector was used as a negative control (Control) in gene overexpression experiments and the lentivirus-mediated empty vector PCDH-CMV-copGFP was used as a negative control (LV-Control) in mouse muscle infection experiments. The data are presented as mean ± SD of three independent experiments; *P < 0.05, **P < 0.01. N.S. indicates statistical non-significance.

of genes such as lncRNA *RP1* (77) and *SATB2-AS1* (78). In our study, the promotion effect of *lncMREF* on myogenic differentiation was inhibited after silencing p300/CBP, implying that the epigenetic regulatory function of *lncMREF* depends on the presence of p300/CBP. However, there is no direct interaction between *lncMREF* and p300, which is consistent with previous reports that p300 tends to fail to interact directly with RNA (79). Further studies revealed that Smarca5 is a bridge between *lncMREF* and p300. Smarca5 binds to *lncMREF* by specifically recognizing the conserved GUA motif of *lncMREF*, while the conserved 482–596 AA domain of Smarca5 is the key region for its binding to the 567–647 AA domain of p300. Smarca5 is a member of the SWI/SNF superfamily and can alter chromatin accessibility (79,80). A recent study demonstrated that *Smarca5* tends to bind to promoters and maintains the accessible chromatin state in Smarca5 binding regions to facilitate the genomic binding of hematopoietic transcription factors in fetal hematopoietic stem and progenitor cells (63). We also found that deletion of *lncMREF* significantly alters chromatin accessibility in target promoter regions and recruits myogenic transcription factors or coactivators, such as p300 and MyoD, to bind to promoters; these results are consistent with the function of *Smarca5*. It is reported that there are quite a few instances of genes that are unimportant for development but turn out to be important for regeneration, such as *TAK1* (81) and *TRAF6* (82). In our study, the expression of *lncMREF* and *Smarca5* increase significantly after the activation of skeletal muscle satellite cells, and their interaction plays an important role in the muscle regeneration. Together, our observations indicated that when satellite cells are activated, *lncMREF* specifically recruits Smarca5 to the target regions and increases chromatin accessibility, which facilitates the genomic binding of p300 or other transcription factors and improves target gene expression.

In summary, we found that *lncMREF* is a specific positive regulator of muscle regeneration among humans, pigs, and mice. Mechanistically, *lncMREF*, whose expression is upregulated by *MyoD*, promotes myogenic differentiation and muscle regeneration by interacting with the Smarca5/p300/CBP complex. When satellite cells are in a resting state, *Smarca5* is expressed at very low levels, and *lncMREF* cannot interact with Smarca5 to regulate the expression of downstream genes. When satellite cells are activated and start to differentiate, Smarca5 is upregulated and recruited by *lncMREF* to their target myogenic regulatory regions, which leads to the upregulation of chromatin accessibility in these target regions. Accessible chromatin increases enrichment of p300/CBP/H3K27ac in myogenic regulatory regions, thereby enhancing myogenic gene expression and muscle regeneration. Our results show for the first time the function of lncRNA-mediated Smarca5/p300/CBP interaction in the specific regulation of muscle regeneration.

DATA AVAILABILITY

The transcriptomics dataset "*lncMREF* KO vs WT" has been deposited at GEO database and is publicly available as of the date of publication. Accession numbers for these datasets are listed in the Supplementary Materials, Table S5. Original/source data are publicly available as of the date of publication. This paper does not report original code. Any additional information required to reanalyze the data reported in this paper is available from the lead contact upon request.

SUPPLEMENTARY DATA

Supplementary Data are available at NAR Online.

REFERENCES

1. Tedesco,F.S., Dellavalle,A., Diaz-Manera,J., Messina,G. and Cossu,G. (2010) Repairing skeletal muscle: regenerative potential of skeletal muscle stem cells. *J. Clin. Invest.*, **120**, 11–19.
2. Ten Broek,R.W., Grefte,S. and Von den Hoff,J.W. (2010) Regulatory factors and cell populations involved in skeletal muscle regeneration. *J. Cell. Physiol.*, **224**, 7–16.
3. Yin,H., Price,F. and Rudnicki,M.A. (2013) Satellite cells and the muscle stem cell niche. *Physiol. Rev.*, **93**, 23–67.
4. Brack,A.S. and Rando,T.A. (2012) Tissue-specific stem cells: lessons from the skeletal muscle satellite cell. *Cell Stem Cell*, **10**, 504–514.
5. Relaix,F. and Zammit,P.S. (2012) Satellite cells are essential for skeletal muscle regeneration: the cell on the edge returns centre stage. *Development*, **139**, 2845–2856.
6. Liu,N., Garry,G.A., Li,S., Bezprozvannaya,S., Sanchez-Ortiz,E., Chen,B., Shelton,J.M., Jaichander,P., Bassel-Duby,R. and Olson,E.N. (2017) A Twist2-dependent progenitor cell contributes to adult skeletal muscle. *Nat. Cell Biol.*, **19**, 202–213.
7. Rugowska,A., Starosta,A. and Konieczny,P. (2021) Epigenetic modifications in muscle regeneration and progression of duchenne muscular dystrophy. *Clin. Epigenet.*, **13**, 13.
8. Tyagi,M., Imam,N., Verma,K. and Patel,A.K. (2016) Chromatin remodelers: we are the drivers!!*Nucleus*, **7**, 388–404.
9. Zhou,C.Y., Johnson,S.L., Gamarra,N.I. and Narlikar,G.J. (2016) Mechanisms of ATP-Dependent chromatin remodeling motors. *Annu. Rev. Biophys.*, **45**, 153–181.
10. Gioacchini,N. and Peterson,C.L. (2017) Chromatin remodeling: a complex affair. *EMBO Rep.*, **18**, 1673–1674.

11. Zhang,X., Wang,X., Zhang,Z. and Cai,G. (2019) Structure and functional interactions of INO80 actin/Arp module. *J. Mol. Cell Biol.*, **11**, 345–355.

12. Kadoch,C., Hargreaves,D.C., Hodges,C., Elias,L., Ho,L., Ranish,J. and Crabtree,G.R. (2013) Proteomic and bioinformatic analysis of mammalian SWI/SNF complexes identifies extensive roles in human malignancy. *Nat. Genet.*, **45**, 592–601.

13. Wee,G., Shin,S.T., Koo,D.B. and Han,Y.M. (2010) Behaviors of ATP-dependent chromatin remodeling factors during maturation of bovine oocytes in vitro. *Mol. Reprod. Dev*, **77**, 126–135.

14. Stopka,T. and Skoultchi,A.I. (2003) The ISWI ATPase snf2h is required for early mouse development. *Proc. Nat. Acad. Sci. U.S.A.*, **100**, 14097–14102.

15. Kokavec,J., Zikmund,T., Savvulidi,F., Kulvait,V., Edelmann,W., Skoultchi,A.I. and Stopka,T. (2017) The ISWI ATPase smarca5 (Snf2h) is required for proliferation and differentiation of hematopoietic stem and progenitor cells. *Stem Cells*, **35**, 1614–1623.

16. Zikmund,T., Kokavec,J., Turkova,T., Savvulidi,F., Paszekova,H., Vodenkova,S., Sedlacek,R., Skoultchi,A.I. and Stopka,T. (2019) ISWI ATPase smarca5 regulates differentiation of thymocytes undergoing β-Selection. *J. Immunol.*, **202**, 3434–3446.

17. Zikmund,T., Paszekova,H., Kokavec,J., Kerbs,P., Thakur,S., Turkova,T., Tauchmanova,P., Greif,P.A. and Stopka,T. (2020) Loss of ISWI ATPase SMARCA5 (SNF2H) in acute myeloid leukemia cells inhibits proliferation and chromatid cohesion. *Int. J. Mol. Sci.*, **21**, 2073.

18. Rossetto,D., Avvakumov,N. and Côté,J. (2012) Histone phosphorylation: a chromatin modification involved in diverse nuclear events. *Epigenetics*, **7**, 1098–1108.

19. Fauquier,L., Azzag,K., Parra,M.A.M., Quillien,A., Boulet,M., Diouf,S., Carnac,G., Waltzer,L., Gronemeyer,H. and Vandel,L. (2018) CBP and P300 regulate distinct gene networks required for human primary myoblast differentiation and muscle integrity. *Sci. Rep.*, **8**, 12629.

20. Puri,P.L., Avantaggiati,M.L., Balsano,C., Sang,N., Graessmann,A., Giordano,A. and Levrero,M. (1997) p300 is required for myod-dependent cell cycle arrest and muscle-specific gene transcription. *EMBO J.*, **16**, 369–383.

21. Roth,J.F., Shikama,N., Henzen,C., Desbaillets,I., Lutz,W., Marino,S., Wittwer,J., Schorle,H., Gassmann,M. and Eckner,R. (2003) Differential role of p300 and CBP acetyltransferase during myogenesis: p300 acts upstream of MyoD and myf5. *EMBO J.*, **22**, 5186–5196.

22. Zhou,J., So,K.K., Li,Y., Li,Y., Yuan,J., Ding,Y., Chen,F., Huang,Y., Liu,J., Lee,W. *et al.* (2019) Elevated H3K27ac in aged skeletal muscle leads to increase in extracellular matrix and fibrogenic conversion of muscle satellite cells. *Aging Cell*, **18**, e12996.

23. Quinn,J.J. and Chang,H.Y. (2016) Unique features of long non-coding RNA biogenesis and function. *Nat. Rev. Genet.*, **17**, 47–62.

24. Li,Y., Chen,X., Sun,H. and Wang,H. (2018) Long non-coding RNAs in the regulation of skeletal myogenesis and muscle diseases. *Cancer Lett.*, **417**, 58–64.

25. Dey,B.K., Pfeifer,K. and Dutta,A. (2014) The H19 long noncoding RNA gives rise to microRNAs miR-675-3p and miR-675-5p to promote skeletal muscle differentiation and regeneration. *Genes Dev.*, **28**, 491–501.

26. Jin,J.J., Lv,W., Xia,P., Xu,Z.Y., Zheng,A.D., Wang,X.J., Wang,S.S., Zeng,R., Luo,H.M., Li,G.L. *et al.* (2018) Long noncoding RNA SYISL regulates myogenesis by interacting with polycomb repressive complex 2. *Proc. Nat. Acad. Sci. U.S.A.*, **115**, E9802–E9811.

27. Yu,X., Zhang,Y., Li,T., Ma,Z., Jia,H., Chen,Q., Zhao,Y., Zhai,L., Zhong,R., Li,C. *et al.* (2017) Long non-coding RNA Linc-RAM enhances myogenic differentiation by interacting with myoD. *Nat. Commun.*, **8**, 14016.

28. Cesana,M., Cacchiarelli,D., Legnini,I., Santini,T., Sthandier,O., Chinappi,M., Tramontano,A. and Bozzoni,I. (2011) A long noncoding RNA controls muscle differentiation by functioning as a competing endogenous RNA. *Cell*, **147**, 358–369.

29. Zhu,M., Liu,J., Xiao,J., Yang,L., Cai,M., Shen,H., Chen,X., Ma,Y., Hu,S., Wang,Z. *et al.* (2017) Lnc-mg is a long non-coding RNA that promotes myogenesis. *Nat. Commun.*, **8**, 14718.

30. Wang,J., Gong,C. and Maquat,L.E. (2013) Control of myogenesis by rodent SINE-containing lncRNAs. *Genes Dev.*, **27**, 793–804.

31. Wang,L., Zhao,Y., Bao,X., Zhu,X., Kwok,Y.K., Sun,K., Chen,X., Huang,Y., Jauch,R., Esteban,M.A. *et al.* (2015) LncRNA dum interacts with dnmts to regulate dppa2 expression during myogenic differentiation and muscle regeneration. *Cell Res.*, **25**, 335–350.

32. Gong,C., Li,Z., Ramanujan,K., Clay,I., Zhang,Y., Lemire-Brachat,S. and Glass,D.J. (2015) A long non-coding RNA, LncMyoD, regulates skeletal muscle differentiation by blocking IMP2-mediated mRNA translation. *Dev. Cell*, **34**, 181–191.

33. Zhang,Z.K., Li,J., Guan,D., Liang,C., Zhuo,Z., Liu,J., Lu,A., Zhang,G. and Zhang,B.T. (2018) A newly identified lncRNA MAR1 acts as a miR-487b sponge to promote skeletal muscle differentiation and regeneration. *J. Cachexia Sarcopenia Muscle*, **9**, 613–626.

34. Li,Z., Cai,B., Abdalla,B.A., Zhu,X., Zheng,M., Han,P., Nie,Q. and Zhang,X. (2019) LncIRS1 controls muscle atrophy via sponging miR-15 family to activate IGF1-PI3K/AKT pathway. *J. Cachexia Sarcopenia Muscle*, **10**, 391–410.

35. Lv,W., Jin,J., Xu,Z., Luo,H., Guo,Y., Wang,X., Wang,S., Zhang,J., Zuo,H., Bai,W. *et al.* (2020) lncMGPF is a novel positive regulator of muscle growth and regeneration. *J. Cachexia Sarcopenia Muscle*, **11**, 1723–1746.

36. Schutt,C., Hallmann,A., Hachim,S., Klockner,I., Valussi,M., Atzberger,A., Graumann,J., Braun,T. and Boettger,T. (2020) Linc-MYH configures INO80 to regulate muscle stem cell numbers and skeletal muscle hypertrophy. *EMBO J.*, **39**, e105098.

37. Cai,B., Li,Z., Ma,M., Wang,Z., Han,P., Abdalla,B.A., Nie,Q. and Zhang,X. (2017) LncRNA-Six1 encodes a micropeptide to activate six1 in cis and is involved in cell proliferation and muscle growth. *Front. Physiol.*, **8**, 230.

38. Dimartino,D., Colantoni,A., Ballarino,M., Martone,J., Mariani,D., Danner,J., Bruckmann,A., Meister,G., Morlando,M. and Bozzoni,I. (2018) The long Non-coding RNA lnc-31 interacts with rock1 mRNA and mediates its YB-1-dependent translation. *Cell Rep.*, **23**, 733–740.

39. Musarò,A. and Carosio,S. (2017) Isolation and culture of satellite cells from mouse skeletal muscle. *Methods Mol. Biol.*, **1553**, 155–167.

40. Li,B.J., Li,P.H., Huang,R.H., Sun,W.X., Wang,H., Li,Q.F., Chen,J., Wu,W.J. and Liu,H.L. (2015) Isolation, culture and identification of porcine skeletal muscle satellite cells. *Asian-Australas. J. Anim. Sci.*, **28**, 1171–1177.

41. He,L., Ding,Y., Zhao,Y., So,K.K., Peng,X.L., Li,Y., Yuan,J., He,Z., Chen,X., Sun,H. *et al.* (2021) CRISPR/Cas9/AAV9-mediated in vivo editing identifies MYC regulation of 3D genome in skeletal muscle stem cell. *Stem Cell Rep.*, **16**, 2442–2458.

42. Livak,K.J. and Schmittgen,T.D. (2001) Analysis of relative gene expression data using real-time quantitative PCR and the 2(-Delta delta C(T)) method. *Methods*, **25**, 402–408.

43. Zhou,L., Sun,K., Zhao,Y., Zhang,S., Wang,X., Li,Y., Lu,L., Chen,X., Chen,F., Bao,X. *et al.* (2015) Linc-YY1 promotes myogenic differentiation and muscle regeneration through an interaction with the transcription factor YY1. *Nat. Commun.*, **6**, 10026.

44. Wei,Y., Li,L., Wang,D., Zhang,C.Y. and Zen,K. (2014) Importin 8 regulates the transport of mature microRNAs into the cell nucleus. *J. Biol. Chem.*, **289**, 10270–10275.

45. Zhang,Y., Li,W., Zhu,M., Li,Y., Xu,Z. and Zuo,B. (2016) FHL3 differentially regulates the expression of MyHC isoforms through interactions with MyoD and pCREB. *Cell. Signal.*, **28**, 60–73.

46. Wang,H., Yang,H., Shivalila,C.S., Dawlaty,M.M., Cheng,A.W., Zhang,F. and Jaenisch,R. (2013) One-step generation of mice carrying mutations in multiple genes by CRISPR/Cas-mediated genome engineering. *Cell*, **153**, 910–918.

47. Hindi,S.M., Shin,J., Gallot,Y.S., Straughn,A.R., Simionescu-Bankston,A., Hindi,L., Xiong,G., Friedland,R.P. and Kumar,A. (2017) MyD88 promotes myoblast fusion in a cell-autonomous manner. *Nat. Commun.*, **8**, 1624.

48. Pasut,A., Jones,A.E. and Rudnicki,M.A. (2013) Isolation and culture of individual myofibers and their satellite cells from adult skeletal muscle. *J. Visual. Exp.*, **73**, 50074.

49. Tosic,M., Allen,A., Willmann,D., Lepper,C., Kim,J., Duteil,D. and Schüle,R. (2018) Lsd1 regulates skeletal muscle regeneration and directs the fate of satellite cells. *Nat. Commun.*, **9**, 366.

50. Guan,H., Zhu,T., Wu,S., Liu,S., Liu,B., Wu,J., Cai,J., Zhu,X., Zhang,X., Zeng,M. *et al.* (2019) Long noncoding RNA LINC00673-v4 promotes aggressiveness of lung adenocarcinoma via activating WNT/β-catenin signaling. *Proc. Nat. Acad. Sci. U.S.A.*, **116**, 14019–14028.

51. Rossi,M., Bucci,G., Rizzotto,D., Bordo,D., Marzi,M.J., Puppo,M., Flinois,A., Spadaro,D., Citi,S., Emionite,L. *et al.* (2019) LncRNA EPR controls epithelial proliferation by coordinating cdkn1a transcription and mRNA decay response to TGF-β. *Nat. Commun.*, **10**, 1969.

52. Wen,S., Wei,Y., Zen,C., Xiong,W., Niu,Y. and Zhao,Y. (2020) Long non-coding RNA NEAT1 promotes bone metastasis of prostate cancer through N6-methyladenosine. *Mol. Cancer*, **19**, 171.

53. Verma,M., Asakura,Y., Wang,X., Zhou,K., Ünverdi,M., Kann,A.P., Krauss,R.S. and Asakura,A. (2021) Endothelial cell signature in muscle stem cells validated by VEGFA-FLT1-AKT1 axis promoting survival of muscle stem cell. bioRxiv doi: https://doi.org/10.1101/2021.08.28.458037, 03 September 2021, preprint: not peer reviewed.

54. Chu,C., Quinn,J. and Chang,H.Y. (2012) Chromatin isolation by RNA purification (ChIRP). *J. Visual. Exp.*, **25**, 3912.

55. Guo,Y., Wang,J., Zhu,M., Zeng,R., Xu,Z., Li,G. and Zuo,B. (2017) Identification of myod-Responsive transcripts reveals a novel long Non-coding RNA (lncRNA-AK143003) that negatively regulates myoblast differentiation. *Sci. Rep.*, **7**, 2828.

56. Pastoret,C. and Sebille,A. (1995) mdx mice show progressive weakness and muscle deterioration with age. *J. Neurol. Sci.*, **129**, 97–105.

57. Spencer,M.J. and Tidball,J.G. (1996) Calpain translocation during muscle fiber necrosis and regeneration in dystrophin-deficient mice. *Exp. Cell. Res.*, **226**, 264–272.

58. Dilworth,F.J., Seaver,K.J., Fishburn,A.L., Htet,S.L. and Tapscott,S.J. (2004) In vitro transcription system delineates the distinct roles of the coactivators pCAF and p300 during myod/E47-dependent transactivation. *Proc. Nat. Acad. Sci. U.S.A.*, **101**, 11593–11598.

59. Lee,J.E., Park,Y.K., Park,S., Jang,Y., Waring,N., Dey,A., Ozato,K., Lai,B., Peng,W. and Ge,K. (2017) Brd4 binds to active enhancers to control cell identity gene induction in adipogenesis and myogenesis. *Nat. Commun.*, **8**, 2217.

60. Polesskaya,A., Naguibneva,I., Fritsch,L., Duquet,A., Ait-Si-Ali,S., Robin,P., Vervisch,A., Pritchard,L.L., Cole,P. and Harel-Bellan,A. (2001) CBP/p300 and muscle differentiation: no HAT, no muscle. *EMBO J.*, **20**, 6816–6825.

61. Puri,P.L., Sartorelli,V., Yang,X.J., Hamamori,Y., Ogryzko,V.V., Howard,B.H., Kedes,L., Wang,J.Y., Graessmann,A., Nakatani,Y. *et al.* (1997) Differential roles of p300 and PCAF acetyltransferases in muscle differentiation. *Mol. Cell*, **1**, 35–45.

62. Vastolo,V., Nettore,I.C., Ciccarelli,M., Albano,L., Raciti,G.A., Longo,M., Beguinot,F. and Ungaro,P. (2018) High-fat diet unveils an enhancer element at the ped/pea-15 gene responsible for epigenetic memory in skeletal muscle. *Metabolism.*, **87**, 70–79.

63. Ding,Y., Wang,W., Ma,D., Liang,G., Kang,Z., Xue,Y., Zhang,Y., Wang,L., Heng,J., Zhang,Y. *et al.* (2021) Smarca5-mediated epigenetic programming facilitates fetal HSPC development in vertebrates. *Blood*, **137**, 190–202.

64. Ulitsky,I., Shkumatava,A., Jan,C.H., Sive,H. and Bartel,D.P. (2011) Conserved function of lincRNAs in vertebrate embryonic development despite rapid sequence evolution. *Cell*, **147**, 1537–1550.

65. Cao,Y., Yao,Z., Sarkar,D., Lawrence,M., Sanchez,G.J., Parker,M.H., MacQuarrie,K.L., Davison,J., Morgan,M.T., Ruzzo,W.L. *et al.* (2010) Genome-wide MyoD binding in skeletal muscle cells: a potential for broad cellular reprogramming. *Dev. Cell*, **18**, 662–674.

66. Soleimani,V.D., Yin,H., Jahani-Asl,A., Ming,H., Kockx,C.E., van Ijcken,W.F., Grosveld,F. and Rudnicki,M.A. (2012) Snail regulates MyoD binding-site occupancy to direct enhancer switching and differentiation-specific transcription in myogenesis. *Mol. Cell*, **47**, 457–468.

67. Martinet,C., Monnier,P., Louault,Y., Benard,M., Gabory,A. and Dandolo,L. (2016) H19 controls reactivation of the imprinted gene network during muscle regeneration. *Development*, **143**, 962–971.

68. Zhao,Y., Cao,F., Yu,X., Chen,C., Meng,J., Zhong,R., Zhang,Y. and Zhu,D. (2018) Linc-RAM is required for FGF2 function in regulating myogenic cell differentiation. *RNA Biol.*, **15**, 404–412.

69. Dong,A., Preusch,C.B., So,W.K., Lin,K., Luan,S., Yi,R., Wong,J.W., Wu,Z. and Cheung,T.H. (2020) A long noncoding RNA, LncMyoD, modulates chromatin accessibility to regulate muscle stem cell myogenic lineage progression. *Proc. Nat. Acad. Sci. U.S.A.*, **117**, 32464–32475.

70. Wang,R., Chen,F., Chen,Q., Wan,X., Shi,M., Chen,A.K., Ma,Z., Li,G., Wang,M., Ying,Y. *et al.* (2022) MyoD is a 3D genome structure organizer for muscle cell identity. *Nat. Commun.*, **13**, 205.

71. Watts,R., Johnsen,V.L., Shearer,J. and Hittel,D.S. (2013) Myostatin-induced inhibition of the long noncoding RNA malat1 is associated with decreased myogenesis. *Am. J. Physiol.-Cell Physiol.*, **304**, C995–C1001.

72. Lin,C. and Yang,L. (2018) Long noncoding RNA in cancer: wiring signaling circuitry. *Trends Cell Biol.*, **28**, 287–301.

73. Tsai,M.C., Manor,O., Wan,Y., Mosammaparast,N., Wang,J.K., Lan,F., Shi,Y., Segal,E. and Chang,H.Y. (2010) Long noncoding RNA as modular scaffold of histone modification complexes. *Science*, **329**, 689–693.

74. Xiang,J.F., Yin,Q.F., Chen,T., Zhang,Y., Zhang,X.O., Wu,Z., Zhang,S., Wang,H.B., Ge,J., Lu,X. *et al.* (2014) Human colorectal cancer-specific CCAT1-L lncRNA regulates long-range chromatin interactions at the MYC locus. *Cell Res.*, **24**, 513–531.

75. Eckner,R., Ewen,M.E., Newsome,D., Gerdes,M., DeCaprio,J.A., Lawrence,J.B. and Livingston,D.M. (1994) Molecular cloning and functional analysis of the adenovirus E1A-associated 300-kD protein (p300) reveals a protein with properties of a transcriptional adaptor. *Genes Dev.*, **8**, 869–884.

76. Zeng,L., Zhang,Q., Gerona-Navarro,G., Moshkina,N. and Zhou,M.M. (2008) Structural basis of site-specific histone recognition by the bromodomains of human coactivators PCAF and CBP/p300. *Structure*, **16**, 643–652.

77. Jia,X., Shi,L., Wang,X., Luo,L., Ling,L., Yin,J., Song,Y., Zhang,Z., Qiu,N., Liu,H. *et al.* (2019) KLF5 regulated lncRNA RP1 promotes the growth and metastasis of breast cancer via repressing p27kip1 translation. *Cell Death. Dis.*, **10**, 373.

78. Wang,Y.Q., Jiang,D.M., Hu,S.S., Zhao,L., Wang,L., Yang,M.H., Ai,M.L., Jiang,H.J., Han,Y., Ding,Y.Q. *et al.* (2019) SATB2-AS1 suppresses colorectal carcinoma aggressiveness by inhibiting SATB2-Dependent snail transcription and epithelial-mesenchymal transition. *Cancer Res.*, **79**, 3542–3556.

79. Shao,L., Sun,W., Wang,Z., Dong,W. and Qin,Y. (2020) Long noncoding RNA SAMMSON promotes papillary thyroid carcinoma progression through p300/Sp1 axis and serves as a novel diagnostic and prognostic biomarker. *IUBMB Life*, **72**, 237–246.

80. Barisic,D., Stadler,M.B., Iurlaro,M. and Schübeler,D. (2019) Mammalian ISWI and SWI/SNF selectively mediate binding of distinct transcription factors. *Nature*, **569**, 136–140.

81. Ogura,Y., Hindi,S.M., Sato,S., Xiong,G., Akira,S. and Kumar,A. (2015) TAK1 modulates satellite stem cell homeostasis and skeletal muscle repair. *Nat. Commun.*, **6**, 10123.

82. Hindi,S.M. and Kumar,A. (2016) TRAF6 regulates satellite stem cell self-renewal and function during regenerative myogenesis. *J. Clin. Invest.*, **126**, 151–168.